RADAR MEASUREMENT OF TURBULENCE IN CONVECTIVE STORMS

by

Ronald Thomas Podsiadlo
B.S., St. Louis University
(1958)

Submitted in Partial Fulfillment
of the Requirements for the
Degree of Master of Science
at the
Massachusetts Institute of Technology
(1965)

Signature of Author. . . . . .
Department of Meteorology
18 January 1965.

Certified by . . . . . .
Thesis Supervisor

Accepted by. . . . . .
Chairman, Department Committee
on Graduate Students

RADAR MEASUREMENT OF TURBULENCE IN CONVECTIVE STORMS

by

Ronald Thomas Podsiadlo

Submitted to the Department of Meteorology on 18 January 1964
in Partial Fulfillment of the Requirements for the
Degree of Master of Science

ABSTRACT

The R-meter is an instrument which gives a direct reading of the variance of the velocity distribution of the scatterers within a radar sampled volume and may thereby provide a method for estimating the magnitude of the turbulence within a storm.

In this study, R-meter measurements were made, utilizing a 10 cm. radar, through fourteen convective storms during the summer of 1964. The measurements yielded rms gust velocities up to 6 m/sec which is the maximum the instrumentation can measure. However, most values remained well below this peak indicating that 6 m/sec is near the highest rms gust velocity to occur in convective storms.

R-meter readings were noted to increase systematically with storm intensities as deduced from measured reflectivities. Highest R-meter readings occurred most frequently at the higher measured elevations.

A model of the basic cell circulation in a single-celled storm was constructed on the assumption that the broad three degree radar beam utilized could detect relative horizontal motion induced by tilted updrafts and downdrafts. The proposed model is similar in structure to Ludlam's model. Turbulent eddies at the interfaces of updrafts and downdrafts were deduced to be the primary source of the higher R-meter readings recorded.

The small sample of data used precluded any firm conclusions. However, the results were encouraging enough to warrant further studies into the use of the R-meter as an instrument for measuring turbulence in convective storms.

Thesis Supervisor: Pauline M. Austin
Title: Senior Research Associate

ACKNOWLEDGEMENTS

The research for this thesis and its preparation was conducted while the author was assigned by the United States Air Force Institute of Technology for graduate training at the Massachusetts Institute for Technology.

The author is indebted to Dr. Pauline Austin for the original suggestion of the topic and wishes to express his sincere thanks for her wise counsel and infinite patience. A note of gratitude is also due the M.I.T. Weather Radar Project for the use of their equipment and facilities with special thanks to the personnel at the radar site, especially to Mr. Spiros Geotis for his invaluable advice and assistance.

TABLE OF CONTENTS

I. INTRODUCTION

Fluctuations in a weather radar signal are caused by relative motions of precipitation particles within the radar sampled volume. These relative motions can be caused by gustiness, wind shear or sedimentation through the volume and only those components of motion parallel to the radar beam can be detected. The fluctuations in the radar signal reveal information about the wind field in the sampled volume if the precipitation particles are assumed to act as reliable tracers of the wind motion.

Hilst (1949) shows that the relative velocity, v, parallel to the radar beam, of two scatterers separated by less than half the pulse length is given in terms of the wave length of the radar signal, λ, and interference frequency, ν, by

$$v = \frac{\lambda \nu}{2} \qquad (1)$$

A pulsed radar, however, can measure unambiguously only those frequencies equal to or less than one-half the pulse repetition frequency (PRF) of the radar (Rogers, 1955).

If the discussion is extended to a whole population of shuffling precipitation particles, there is now not just the one frequency returned but a spectrum, the shape of which is determined by the amount of power returned for each detected relative velocity. The sprectrum itself, however, is not the probability distribution of relative velocities. Fleisher (1953) has shown rigorously that the correct velocity distribution is obtained by transforming the power spectrum to the time

domain through use of the Fourier integral

$$g^2(\tau) = \int_{-\infty}^{\infty} F(\omega) e^{i\omega\tau} d\omega \qquad (2)$$

where $g^2(\tau)$ is the autocorrelation of power, $F(\omega)$ is the power spectrum, and ω is the angular frequency.

The function $g(\tau)$ $(\equiv \sqrt{g^2(\tau)})$ is tranformed back to the frequency domain by the Fourier transform,

$$f(\omega) = \frac{1}{2\pi} \int_{-\infty}^{\infty} e^{-i\omega\tau} g(\tau) d\tau \qquad (3)$$

where $f(\omega)$ may be converted from angular frequency to cycles per second and then through equation (1) directly to the desired velocity distribution.

Stone and Fleisher (1956) used the above approach and with the aid of a computer derived several gust velocity distributions from weather noise data. They assumed negligible wind shear effects since a beam width of only 500 feet was used in the measurements. This technique required that the target characteristics remain unaltered during an observation. They therefore applied the condition that the average value of the returned signal remain constant during measurement with the result that only relatively short records were attainable. Consequently, conclusions about time series of assumed infinite duration had to be made after just a few moment's scrutiny. Their results were therefore hard to obtain and subject to great error.

A measurement of gustiness, or at least of signal fluctuations, can be made much more quickly with an instrument called the R-meter. The R-meter, described by Rutkowski and Fleisher (1955), simply measures

the number of times the signal crosses a selected level, usually chosen as the average signal amplitude. They show that the number of crossings is directly proportional to the variances of gustiness, wind shear, and sedimentation within the radar sampled volume. Although the R-meter makes a quick direct measurement, it gives only thevariance, not the entire velocity distribution.

Some analyses of R-meter measurements have been made. Rogers (1957) describes the uses and operation of the R-meter and presents some results from measurements made in widespread rain or snow. He tried to measure gustiness by subtracting out the wind shear contribution through comparison with radiosonde data. He discusses also the performance of the instrument and its limits of accuracy. Stackpole (1959) extended the studies of Fleisher (1957) on the variation in time of the intensity of turbulence at a particular location. He used long records of R-meter data taken in uniform precipitation of a warm or occluded frontal nature. He assumed that wind shear contributed average values to the readings and variations were caused by turbulent eddies passing through the stationary sampled volume. From spectrum analyses of the data, he draws some conclusions as to the turbulence structure of the atmosphere. Since the techniques Rogers and Stackpole used required either observing over relatively large areas or for long times, they were largely restricted to observations in stratiform precipitation. They both used the AN/CPS-9 radar in their studies with the R-meter.

This study proposes to make R-meter measurements through convective storms in an attempt to determine the distribution and intensity

of turbulence within the storms. Environmental wind shear is assumed to affect only slightly the motion of particles within the storm. This assumption is supported by the vertical appearance of convective storm cores in RHI photos, and by the absence of a bright band which indicates that vertical motions prevent the uniform falling out of hydrometeors. Effects of sedimentation are also neglected since measurements are made at elevations less than ten degrees. Simultaneous measurements of signal intensity are also made to determine whether any relationship exists between intensity of turbulence and amount of liquid water or hail in the storm.

II. INSTRUMENTATION

A. Radar:

The SCR-615B weather radar located at Massachusetts Institute of Technology (42°22'N, 71°06'W) was used for all R-meter measurements made in this study. The SCR-615B radar has a wave length of 10.7 centimeters, a conical beam three degrees between half-power points, a pulse length of 450 meters, and it normally operates on a PRF of 400 cps. For comparison, the radar used in previous studies with the R-meter, the AN/CPS-9, has a 3.2 centimeter wave length, a one degree conical beam, a pulse length of 150 meters and operates on a PRF of 931 cps.

The severe attenuation experienced by the three centimeter radar in intense storms made its use in this study prohibitive. This is the primary reason for using the non-attenuating ten centimeter radar. Another advantage is found in its ability to detect higher relative velocities than the three centimeter radar because of its longer wave length. This becomes clear when we replace v in equation (1) with one-half the pulse repetition frequency (pulsed radars) and solve for the maximum detectable relative velocities for the two wave lengths. For the AN/CPS-9 radar, we have

$$v_{max} = \frac{\lambda\left(\frac{1}{2}PRF\right)}{2} = \frac{3.2(465)}{2} = 7.4 \text{ m/sec}$$

For the SCR-615B radar, we have,

$$v_{max} = \frac{10.7(200)}{2} = 10.7 \text{ m/sec}$$

To broaden the range of detectable relative velocities even further,

the PRF was increased to 667 cps for most measurements. This increases v_{max} to 17.8 m/sec which is more than twice that detectable by the AN/CPS-9 radar.

An apparent disadvantage of the SCR-615B radar is its large three degree beam which increases the sampled area to nine times that of the one degree beam. (See Figure 1). Since all the relative motions within and along the beam are integrated and measured indiscriminately, the larger beam allows much less resolution than is possible with the smaller beam.

The depth of the SCR-615B's sampling volume is 300 meters which is determined by taking one-half the pulse length, 225 meters, and adding to it the sampling gate length of 75 meters. This is twice the depth of the AN/CPS-9's sampling volume.

B. R-Meter:

The R-meter is an instrument which measures the rate at which a fluctuating radar signal reaches or crosses any selected voltage level. Rutkowski and Fleisher (1955) show that the rate of level crossings, W, is related to the variance, σ^2, as follows,

$$\sigma_g^2 + \sigma_s^2 + \sigma_f^2 = \frac{\pi W^2}{4\left(\frac{4\pi}{\lambda}\right)^2} \frac{I_o e^{\frac{2A^2}{I_o}}}{A^2} \qquad (4)$$

where,

σ_g^2 = the variance of the gustiness

σ_s^2 = the variance of the vertical wind shear

σ_f^2 = the variance of the sedimentation

I_o = the average signal intensity across a 1 ohm resistance

A = the selected voltage level

W = the rate of level crossings

λ = the wave length of the radar signal

The ratio $\frac{A^2}{I_o}$ is difficult to obtain readily. However, it is possible to read the rate of level crossings at the average value of the signal without knowing explicitly what the value is. In this case,

$$A = \frac{1}{2}\sqrt{\pi I_o} \qquad (5)$$

Substituting this for A in equation (4) yields

$$\sigma_g^2 + \sigma_s^2 + \sigma_f^2 = \left[\left(\frac{\lambda}{4\pi}\right)^2 e^{\frac{\pi}{2}}\right] W^2 \qquad (6)$$

But, since the quantity $\left(\frac{\lambda}{4\pi}\right)^2 e^{\frac{\pi}{2}}$ depends only on wave length, we can write,

$$\Sigma\sigma^2 = kW^2 \qquad \text{where} \qquad K = \left(\frac{\lambda}{4\pi}\right)^2 e^{\frac{\pi}{2}}$$

For λ = 10.7 cm., K = 3.47 cm^2. Therefore, for the SCR-615B radar,

$$\Sigma\sigma^2 = 3.47\,W^2 \qquad (7)$$

The electronic apparatus which measures the rate of level crossings, W, records these crossings, as they occur, on an Esterline Angus Recorder. The recorder is set such that $W = 4 \times EA$ where EA represents the Esterline Angus chart reading.

As an example, for an EA of 30, W = 4 x 30 = 120 level crossings per second. The sum of the variances is then,

$$\Sigma\sigma^2 = 3.47\ (120)^2 = 5 \times 10^4\ cm^2\ sec^{-2}$$

The square root of the sum of the variances gives an estimate of the root mean square (rms) gust velocity. In this case,

$$\sqrt{\Sigma\sigma^2} = 224 \text{ cm/sec}$$

Rogers (1957) has discussed the limitations of the R-meter. He shows how, at low signal intensities, receiver noise introduces spurious level crossings to the R-meter readings, yielding higher fluctuation rates than are really present in the sampled region. Another limitation is imposed by the PRF of the radar which sets an upper limit to the number of level crossings that can be measured by the R-meter. At a PRF of 400 cps, this limit lies near 200 level crossings per second ($EA = 50$), while at a PRF of 667, it rises to near 320 crossings per second ($EA = 80$). Clearly, the higher PRF is to be preferred for taking R-meter measurements. ROgers (1957) made a few measurements in shower activity and obtained a maximum rms gust velocity of 1.5 m/sec which was near the limit that his instrumentation could measure. In this study, the maximum detectable rms gust velocity, using a PRF of 667 cps, is 6 m/sec.

Although it is probable that the major contribution to the R-meter readings in convective storms is turbulence, there is no way of knowing for certain the size of the eddies involved. Rogers (1957) deduced that an eddy equal in size to the sampled volume would be most effective in producing detectable relative velocities. He adds, however, that smaller eddies of sufficient density to utilize all the scatterers within the volume would be equally effective. Therefore, with the large three degree beam used in this study, the R-meter may be measuring

relative velocities caused by anything from small eddies to the basic internal cell circulation, provided the latter has significant horizontal components, that is, tilted updrafts and downdrafts.

C. Pulse Integrator:

The pulse integrator utilizes the same sampling gate as the R-meter and measures the average value of the fluctuating signal from the sampled volume. The average is taken over a period of approximately one-half second. This average signal is recorded on an Esterline Angus Recorder whose readings can be converted to signal intensity values in decibels below a milliwatt (dbm) after calibration. Simultaneous time marks can be placed automatically on both the R-meter and pulse integrator records for subsequent reference during analysis.

D. Profile Plotter:

The profile plotter is a time and labor saving device that can be attached to the radar's R-Scope. At the flip of a switch, the plotter automatically sweeps the sampling gate through the echo of interest and records the two-mile range markers simultaneously on both EA recorders as the markers are traversed on the R-scope. After each run through an echo, a new run at a different elevation can be started within a few seconds. The speed with which the gate traverses an echo can be varied anywhere from one mile in three seconds to one mile in fourteen seconds.

III. OBSERVING TECHNIQUES

The basic measurements made in this study are simultaneous R-meter and pulse integrators runs through the cores of convective storms at different elevation angles. From these data, cross sectional profiles are constructed showing the fluctuation rates and the simultaneous signal intensities occurring at the different elevations through the storms.

For a few fast moving storms, the sampling gate was held fixed and the storm allowed to move through the sampling volume. This technique proved too time consuming and yielded dubious results since local time variations of turbulence were suspected to distort the desired spatial variations through the storm.

With the profile plotter, sampling gate speeds of one mile in ten to twelve seconds were used in most measurements. These speeds are slow enough to allow a sufficient number of pulses to intercept each sampled volume. For example, a gate speed of one mile in ten seconds (528 ft/sec) traverse the SCR-615B sampling volume length of 985 feet in 1.86 seconds. If a PRF of 667 cps is used, 1240 pulses intercept each sampled volume as the gate passes through. This is more than adequate for representative sampling. Also, these speeds are fast enough to allow several profiles to be taken through a storm during the same stage in its life history. With a little practice, runs at three different elevation angles can be made through a storm six miles in diameter in less than five minutes.

The relatively short time required for a complete profile makes it possible to obtain adequate data without seriously interfering

with other required radar measurements. In particular, sequences of intensity contours on PPI are required at intervals no longer than ten minutes. These PPI sequences are vital adjuncts to the R-meter data. From them, it is possible to determine the stage in a storm's life cycle at the time of the R-meter run and also the direction of motion of the storm with respect to the orientation of the cross section.

All measurements were made on storms within fifty miles to keep the size of the sampled volume below a reasonable maximum. Also, very few measurements were taken within fifteen miles due to interference from ground clutter.

The R-meter profiles were constructed by drawing smooth curves through the average values of the fluctuating EA traces. (Figure 2). These curves were then carefully copied onto graph paper above their corresponding signal intensity traces.

IV. DESCRIPTION OF THE DATA

Data collection began on 24 June, 1964 and ended on 26 August, 1964. During this period, reliable measurements were made through fourteen storms. During the earlier measurements, instrumentation and observing techniques were still unpolished, so coverage is not as complete as could be desired. The storm of 6 July (Figure 3c) is the only one shown in which the sampling gate was held fixed during measurement. This is also the only storm presented where a PRF of 400 cps was used during the measurements. All other data was taken utilizing a PRF of 667 cps. Measurements through the two storms of 1 July (Figures 3a and 3b) were taken by cranking the range gate through the storm manually. The profile plotter was used in the remainder of the storms.

The resultant R-meter and pulse integrator profiles through these storms and their corresponding PPI intensity contour representations nearest to measurement times are shown in Figure 3-12. Each PPI representation shows the line of observation through the storm and the direction and speed of the storm. The R-meter readings are given in EA units which can be converted to rms gust velocities, , by the formula,

$$7.43 \times EA = \sigma_g \quad (\text{cm/sec})$$

This relationship assumes negligible contribution to the total variance from wind shear and sedimentation.

The signal intensity values are given in dbm units (decibels below a milliwatt) normalized to a range of one mile. The dbm values,

P_r, may be converted to <u>equivalent</u> radar reflectivity values, Z_e,* by applying the equation,

$$10 \text{ Log } Z_e = -P_r + 85$$

For example, a P_r value of 35 dbm yields a value of 10^5 mm^6/m^3 for Z_e. The Z_e values can give a rough estimate of equivalent rainfall rates by the empirical formula,

$$Z_e = 200 R^{1.6}$$

where R is in mm/hr. As an example, for $Z_e = 10^5$ mm^6/m^3, $R \approx 50$ mm/hr, or for $Z_e = 10^3$ mm^6/m^3, $R \approx 3$ mm/hr.

These relationships are valid assuming that the beam is filled with liquid water drops and not ice particles. Liquid water is found to be the dominant hydrometeor in most thunderstorms up to 20,000 feet. Since the great majority of measurements in this study are at or below this level, the relationships given are generally applicable to the data.

* The radar reflectivity factor, Z, is defined as the sum of the sixth powers of the diameters of all the precipitation particles in a unit volume of the sampled region. If the particles are small compared with the wave length of the radar (as is true in this study), Z is an accurate measure of the radar echo reflectivity.

V. DISCUSSION OF THE DATA

A. General:

Overall, the profiles reveal no apparent systematic pattern. Both R-meter and pulse integrator profiles have a wide variety of structure with peaks in the two traces seeming to occur randomly with respect to one another. There is noted, however, a clear tendency for the higher fluctuation rates to occur at the higher elevations. The effect of receiver noise is readily seen in the apparent increase in fluctuation rates near the edges of most storms. An example of this is evident in Figure 6a.

A closer inspection of the data reveals a tendency for the higher fluctuation rates to occur in the more intense storms. This is noted particularly in the 1 July storm (Figure 3b) where the highest signal intensities and fluctuation rates of the summer were recorded prior to 26 August. This storm produced 1/4 - 3/4 inch hail at the ground, strongly suggesting that the R-meter was indeed recording the heavy turbulence suspected to be associated with hailstorms. A scatter diagram was constructed with a plot of the highest R-meter reading versus the highest signal intensity to occur in any part of each storm (Figure 13a). All points but the two 26 August readings fall near the line drawn in the diagram, supporting the premise that increasing intensity means increasing turbulence in storms. The very high fluctuation rates attained in the 26 August storms despite their moderate intensity are very probably real. However, there is a slight possibility that a flaw in the instrumentation or an error in the signal calibration may have produced these results. Further measurements are needed to

determine for certain whether this phenomenon does really occur and under what conditions it occurs.

When plots were made of the highest corresponding values of signal intensity and EA readings to occur at individual levels, no similar correlation was found (Figure 13b). This does indicate, however, that intense precipitation at any level in a storm suggests the presence of strong turbulence, but not necessarily at that same level. A review of the profiles shows that in all cases the highest fluctuation rates occur either at the same elevation or at a higher elevation than the highest signal intensities.

A scatter diagram was made with a plot of minimum R-meter readings versus maximum signal intensities at the same elevations through the storms (Figure 14a). Again, the scatter is random, but the diagram does suggest that fluctuation rates tend to remain relatively high at the higher elevations regardless of storm intensity.

The effects of the large three degree beam on the results were tentatively tested by plotting all R-meter readings versus range at one mile increments. The results (Figure 14b) reveal no pattern except, perhaps, for the lowest readings to occur at lesser ranges and a slight tendency for the highest readings to occur at greater ranges. This may be a result of the broadening of the beam at greater ranges but no firm comment can be made in view of the very great scatter noted.

B. Cell Circulation Deduced from R-Meter Data - A Case Study:

It is suspected that when conditions are right, the broad beam of the SCR-615B radar may allow the R-meter to detect the basic cell

circulation in a thunderstorm. If Ludlam's model (1963) is assumed (Figure 15), the tilted drafts might yield sufficient horizontal components of relative motion to be detected by the R-meter. These components could best be seen if the storm were moving directly towards or away from the radar beam. In addition, it is desirable that the storm be fairly intense and single-celled in order that the circulation be strong and clearly defined as in Ludlam's model.

These conditions were fortuitously met on 23 July, 1964. On that morning, an east-west cold front, drifting slowly across southern New England, touched off several thunderstorms to the south of the radar site. The surface streamlines and the radar echo position at 1100 EST are shown in Figure 16. The storm at 202 degrees and 35 miles (arrow) is the subject of this case study.

At 0953 EST, this storm was centered at 210° and 28 miles and was made up of three cells of moderate intensity (Figure 7a). The storm drifted south-southeastward at about five miles per hour and by 1040 EST was centered at 202° and 32 miles (Figure 17a). It had increased slightly in size and now had a two-cell structure. Just five minutes later, at 1045 EST (Figure 17b), the storm had rapidly organized itself into one large cell and reached its peak intensity, $Z_e = 10^{5.2}$ mm^6/m^3, the highest recorded in any cell that day. R-meter and pulse integration runs at elevations of one, three, five and seven degrees were taken through this cell beginning at 1050 EST and ending at 1058 EST. The storm's structure after this run is shown in Figure 17c. The intensity had decreased and the structure was no longer well defined. The storm's position at this time shows a change in direction to the

south-southwest and an increase in speed to ten miles per hour directly along and away from the line of observation. The relatively slow speed of the storm facilitated measurement using the profile plotter and minimized range corrections in the subsequent analysis needed to allow for storm motion between each elevation run.

Thus, all the desired conditions were met to test the foregoing hypothesis. The R-meter and pulse integrator profiles through the storm are shown in Figure 18. The pulse integrator traces clearly indicate the basic single-celled structure with the absence of minor peaks suggesting the steady state condition proposed by Ludlam (1963). That the pulse integrator is capable of detecting minor peaks in signal intensity is clearly illustrated in Figure 6a. These are profiles through this same storm taken one hour earlier while it was made up of several cells.

A cross section of the storm's structure was fashioned by plotting signal intensities in 5 db intervals at their appropriate positions along the center line of the beam at each elevation angle. Lines of equal intensity were then drawn to obtain the pattern shown in Figure 19a. The upright rectangle in the figure are side views of the radar sampling volumes centered at the points along each beam where the peaks in the R-meter traces occurred. Both the signal intensity values and positions of the R-meter peaks were range corrected to account for storm motion.

At this point, the assumption that the R-meter can detect relative motions caused by the wind shear induced by tilted up and down drafts is applied. With this in mind, the cell circulation depicted in Figure 19b was constructed.

The lines of maximum shear, that is, where the vertical velocities drop to zero above and below the updraft's central maximum, were drawn through the centers of the sampling volumes in the figure. These are the points where it would seem that maximum relative motions would occur through the vertical extent of the beam at each elevation. It will be noted that the updraft core intersects either the top or bottom third of these four sampling volumes. The updraft, as constrcuted, is tilted at an angle of 50° with the horizontal. Above the main updraft, winds are relatively light and directed towards the front of the storm as in Ludlam's model. Below the updraft, general downward motion is occurring with a component towards the front of the storm induced by air rushing in from the rear of the storm at its middle and lower levels. These factors all tend to maximize relative horizontal motions at the points chosen. The minor peak at 32.6 miles and three degrees elevation is interpreted as being the region where the main updraft first overturns at its base and becomes a part of the downdrafts in the lower portions of the storm. The breakdown of the main updraft in the rear half of the storm marks the beginning of the dissipation stage as suggested in the PPI representations. The axis of maximum overturning (dash-dot line) is tilted up to the rear of the storm to account for the gradual decrease in, yet relatively high readings along the three-degree elevation line. The absence of any other significant R-meter peaks is supported in this model by the corresponding absence of any other vigorous drafts to induce strong shear across any of the elevations at which measurements were made.

Another significant feature supporting the model is the position of the storm's core immediately beneath the region where the main updraft first begins to diverge towards the rear and upper parts of the storm. It is suggested that the sudden decrease in vertical velocities due to this spreading out of the updraft causes release of the larger liquid water drops being supported in the draft. Also, the core lies beneath the region where the diverging updrafts have maximum vertical components to support maximum condensation.

A final note of support is found in the indentation of the signal intensity contours in the lower levels at the front edge of the storm which fits nicely with the depicted circulation pattern.

A very rough comparison can be made between the measured rms gust velocities and estimated draft velocities in this model. The maximum rms gust velocity measured was 4.8 meters per second. Braham (1952) has indicated that updraft velocities on the order of 30 feet per second are reasonable for fairly vigorous storms. Assuming this is the vertical component of the tilted updraft velocities, the horizontal components, for a draft tilted at 50° to the horizontal , would be 25 feet per second or 8 meters per second. Rogers (1957) derived the following expression for the variance of the vertical wind shear assuming linear shear across the beam,

$$\sigma_s^2 = \frac{u_o^2}{4}$$

where is defined as half the wind shear.

The square root of the variance yields an estimate of the rms velocity, or

$$\sigma = \frac{u_o}{2}$$

Now, consider the sampling region in Figure 19b that depicts a peak at 33.5 miles and 3° elevation. Assume that the horizontal component of the updraft velocity decreases from 8 m/sec at the top of the beam (center of the updraft) to zero at the center of the beam (base of the updraft). The horizontal components of motion below the updraft are relatively light and may be assumed to increase slowly to a maximum of 2 m/sec in the opposite direction at the bottom of the beam. A rough estimate of the wind shear across the height of the beam would therefore be near 10 m/sec. Since U_0 is one-half the wind shear or 5 m/sec, the estimated rms velocity is therefore one half this value or 2.5 m/sec. This is roughly half the value obtained by R-meter measurement (4.8 m/sec).

Despite the assumptions and rough estimates made and the fact that the measured and estimated rms velocities are of the same order of magnitude, it is likely that the result obtained is at least in the reight direction. That is, the vertical wind shear induced by tilted drafts contributes only a portion of the total variance. The additional and probably primary source of relative motions is suspected to be found in the turbulent eddies at the interfaces of the updrafts and downdrafts. This is said in view of the high R-meter readings obtained even when a storm was not moving along the beam. (See. Figures 11c and 12c)

VI. CONCLUSIONS

The highest rms gust velocity which can be measured by a 10.7 cm wave length radar on a PRF of 667 cps is about 6 meters/sec. This is believed to be near the maximum value to occur in most convective activity since all but a few measurements taken in this study remained well below it. This upper limit was approached or reached only in storms which had very high reflectivities and were believed to contain large hail.

Fluctuation rates systematically increase with storm intensity with highest rates occurring almost invariably at the higher measured elevations regardless of storm intensity.

It is suspected that the broad beam of the SCR-615B radar permits the measurement of the basic circulation of a single-celled storm if it contains up and down drafts that are tilted along the radar beam. The 23 July case study lent strong support to this hypothesis as the deduced cell circulation bore a remarkable resemblance to that in Ludlam's model.

The fact that equally high fluctuation rates were recorded even when the motion of the storm was not along the beam strongly suggests that turbulent eddies along the interfaces of the updrafts and downdrafts are the primary source of high fluctuation rates with the effects of tilted drafts playing a secondary role.

Paucity of data precludes making firm conclusions about any of the results. Many more measurements are needed to either affirm or discount any trends or proposals noted in this report.

VII. SUGGESTIONS FOR FUTURE RESEARCH

The effects of the broad beam used in this study can best be evaluated by comparison with similar measurements made with a ten centimeter radar utilizing a one degree beam. Systematically lower readings with the smaller beam would suggest eddies more comparable in size to the larger beam and vice versa.

The impossibility of making measurements through a storm from orthogonal directions is frustrating. The best that can be done at present is comparison of many measurements through many storms with respect to the direction of storm motion. Such comparisons might yield clues as to the orientation, extent and intensity of turbulent eddies within a storm with respect to the storm's motion, intensity, size or any other characteristic.

If a narrower beam were used, cranking the range gate through a storm azimuthally might reveal the lateral extent of eddies detected radially at a particular azimuth.

R-meter studies of relatively weak convective activity will have to be made with a shorter wave length radar or a more sensitive one since receiver noise interferes with readings made through weak showers with the SCR-615B radar.

Further investigation into the validity of deducing cell circulation from R-meter data should be made by taking measurements of the type described whenever possible and seeing if similar patterns of peaks in the fluctuation rates are consistently obtained.

The ideal set-up for evaluating R-meter data is virtually unattainable. The set-up would include simultaneous readings through the

same storm with both one and three degree beams and from aximuths along and perpendicular to the storm's motion. In addition, simultaneous PPI and RHI pictures would be taken using one degree beams. Even if this elaborate arrangement were possible, it is doubtful that the resultant R-meter data would yield enough reliable information to determine the complete turbulence structure of a convective storm. There are too many uncertainties involved which are inherent in the R-meter instrumentation. In particular, the integration of all relative velocities in the beam, regardless of their position or origin, make evaluation of the data particularly uncertain.

On the other hand, numerous carefully made and carefully evaluated measurements of the type suggested are still quite capable of revealing much useful information on the general turbulence structure and intensity in convective storms when considered in the light of the instrument's capabilities as well as its limitations.

REFERENCES

Braham, R.R., Jr. 1952: The Water and Energy Budgets of the Thunderstorm and Their Relationship to Thunderstorm Development. J. Meteo., 9, pp. 227-242.

Browning, K.A. and F.H. Ludlam, 1962: Airflow in Convective Storms. Quart. J.R. Meteo., 88, pp. 117-135.

Byers, H. R. and R.R. Braham, Jr., 1948: Thunderstorm Structure and Circulation. J. Meteo., 5, pp. 71-86.

Fleisher, A., 1953: The Information Contained in Weather Noise. Weather Radar Res. Rep. No. 22, Dept. of Meteor., Mass. Inst. of Tech.

————————, 1957: Some Spectra of Turbulence in the Free Atmosphere. Weather Radar Res. Rep. No. 31, Dept. of Meteor, Mass. Inst. of Tech.

Hilst, G.R., 1949: Analysis of Audio-Frequency Fluctuations in Radar Storms Echoes: A Key to the Relative Velocities of the Precipitation Particles. Weather Radar Res. Rep. No. 9, Dept. of Meteor., Mass. Inst. of Tech.

Ludlam, F.H., 1963: Severe Local Storms: A Review. Meteor. Monogr., 5, pp. 1-30.

Rogers, R.R., 1957: Radar Measurement of Gustiness. Weather Radar Res. Rep. No. 29, Dept of Meteor., Mass. Inst. of Tech.

Rutkowski, W. and A. Fleisher, 1955: R-Meter: An Instrument for Measuring Gustiness. Weather Radar Res. Rep. No. 24, Dept. of Meteor., Mass, Inst. of Tech.

Stackpole, J.D., 1959: Radar Measurement of the Spectra of Turbulence in the Free Atmosphere. Weather Radar Res. Rep. No. 32, Dept. of Meteor., Mass. Inst. of Tech.

Stone, M.L., and A. Fleisher, 1956: Measurement of Weather Noise. Weather Radar Res. Rep. No. 26, Dept. Meteor., Mass. Inst. of Tech.

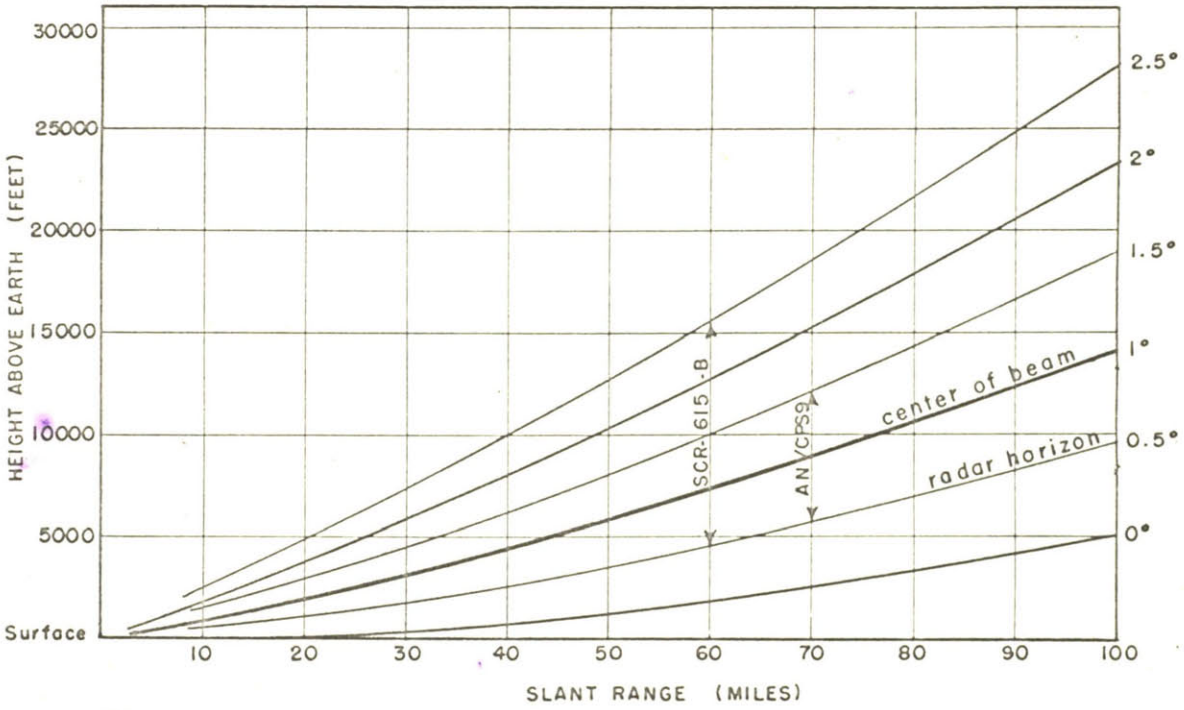

Figure 1. Range-Height Diagram showing difference in beam widths between SCR-615B and AN/CPS-9 radars.

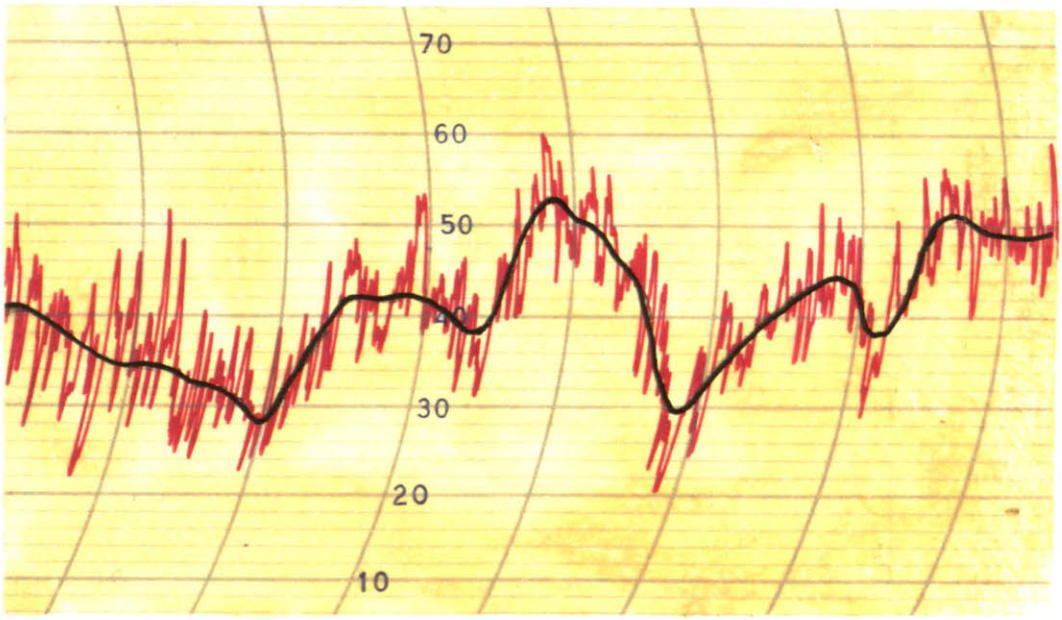

Figure 2. Sample R-meter trace with smooth curve drawn through average values.

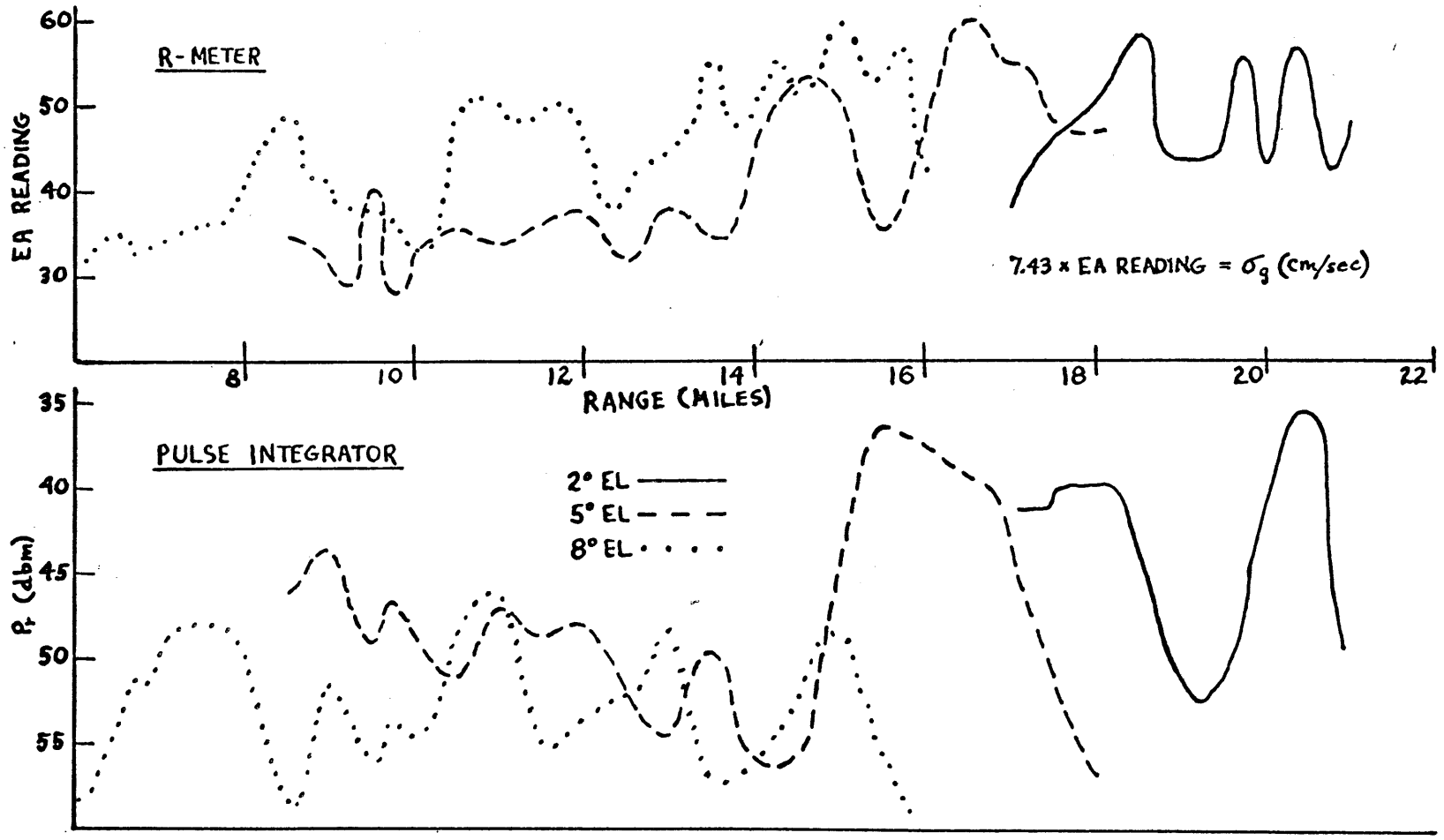

Figure 3a. Profiles for 1 July, 1400-1415 EST, 319° Azimuth. (See Figure 4a). Pr values (dbm) may be converted to Ze values using 10 Log Ze = - Pr + 85. Equivalent rainfall rates, R, may be estimated by using $Ze = 200R^{1.6}$ (R in mm/hr).

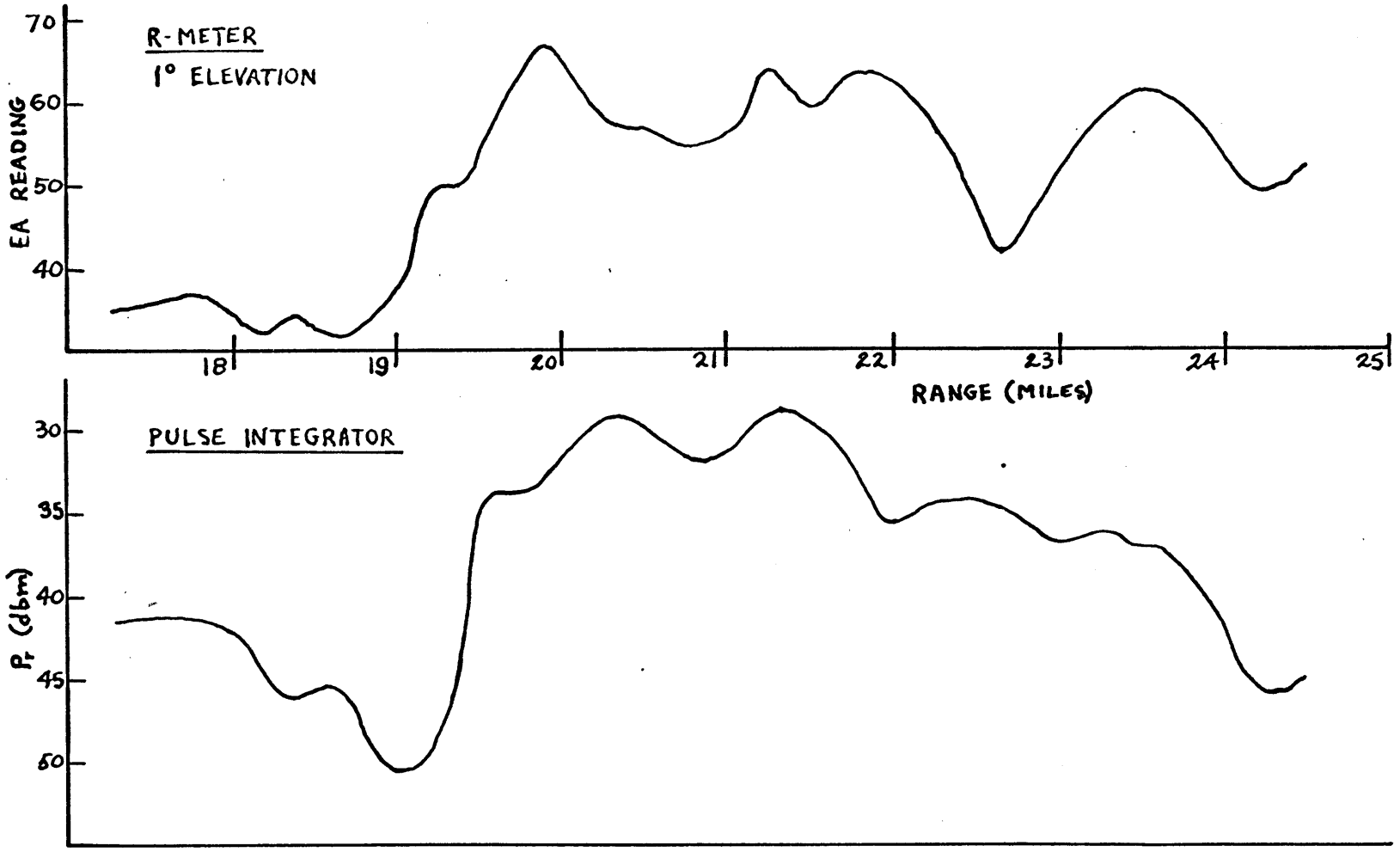

Figure 3b. Profiles for 1 July, 1628-1632 EST, 215° Azimuth. (See Figure 4b).

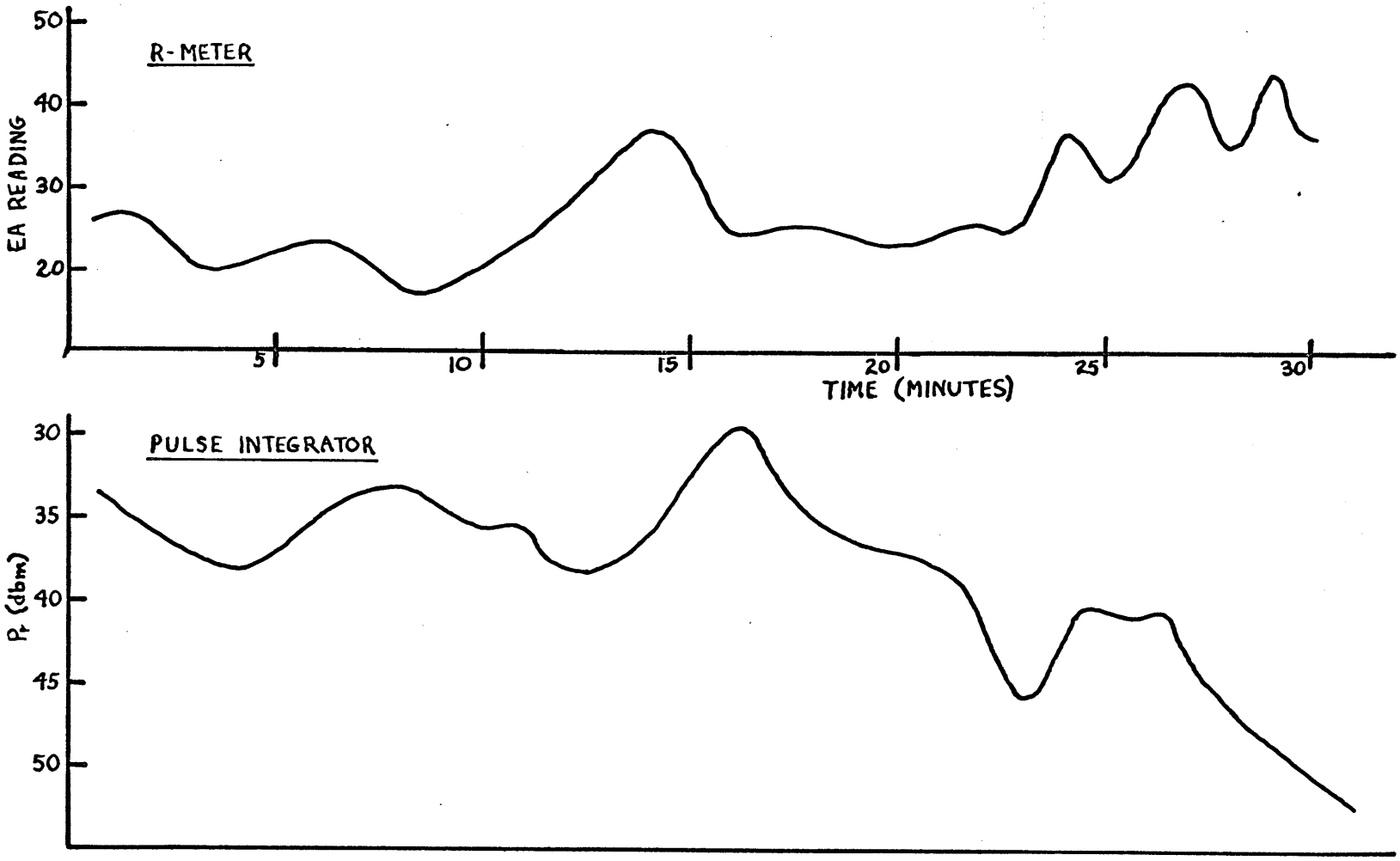

Figure 3c. Profiles for 6 July, 1547-1617 EST. Sampling gate held fixed at 290°/17.3 miles and 1° elevation. (See Figure 4c). PRF of 400 cps used. All other data utilized a PRF of 667 cps.

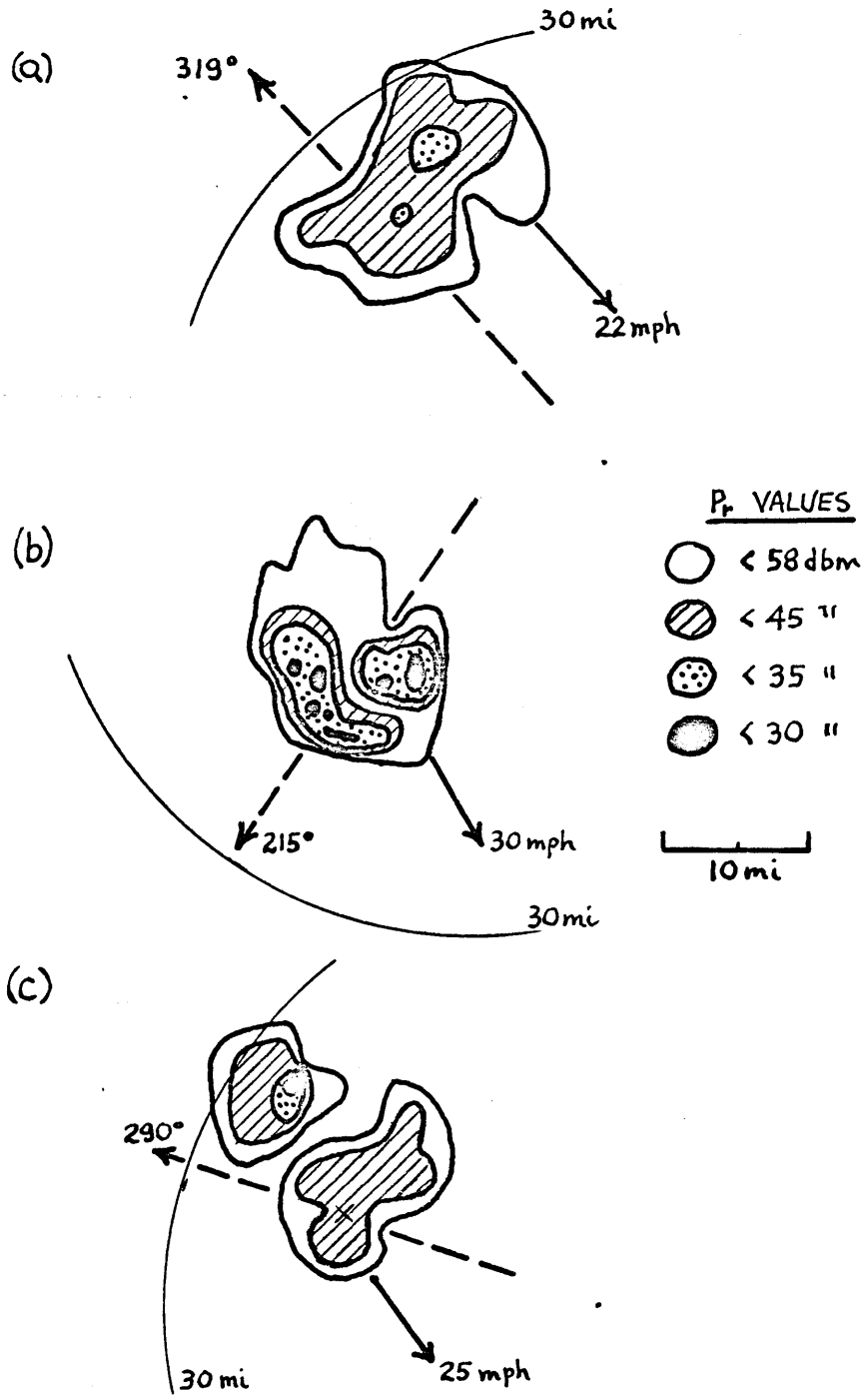

Figure 4. PPI intensity contours. (a) 1 July, 1353 EST. (b) 1 July 1649 EST. (c) 6 July 1535 EST. Dashed arrows show line of observation during R-meter and pulse integrator measurements. Solid arrows show direction of motion and speed of storm.

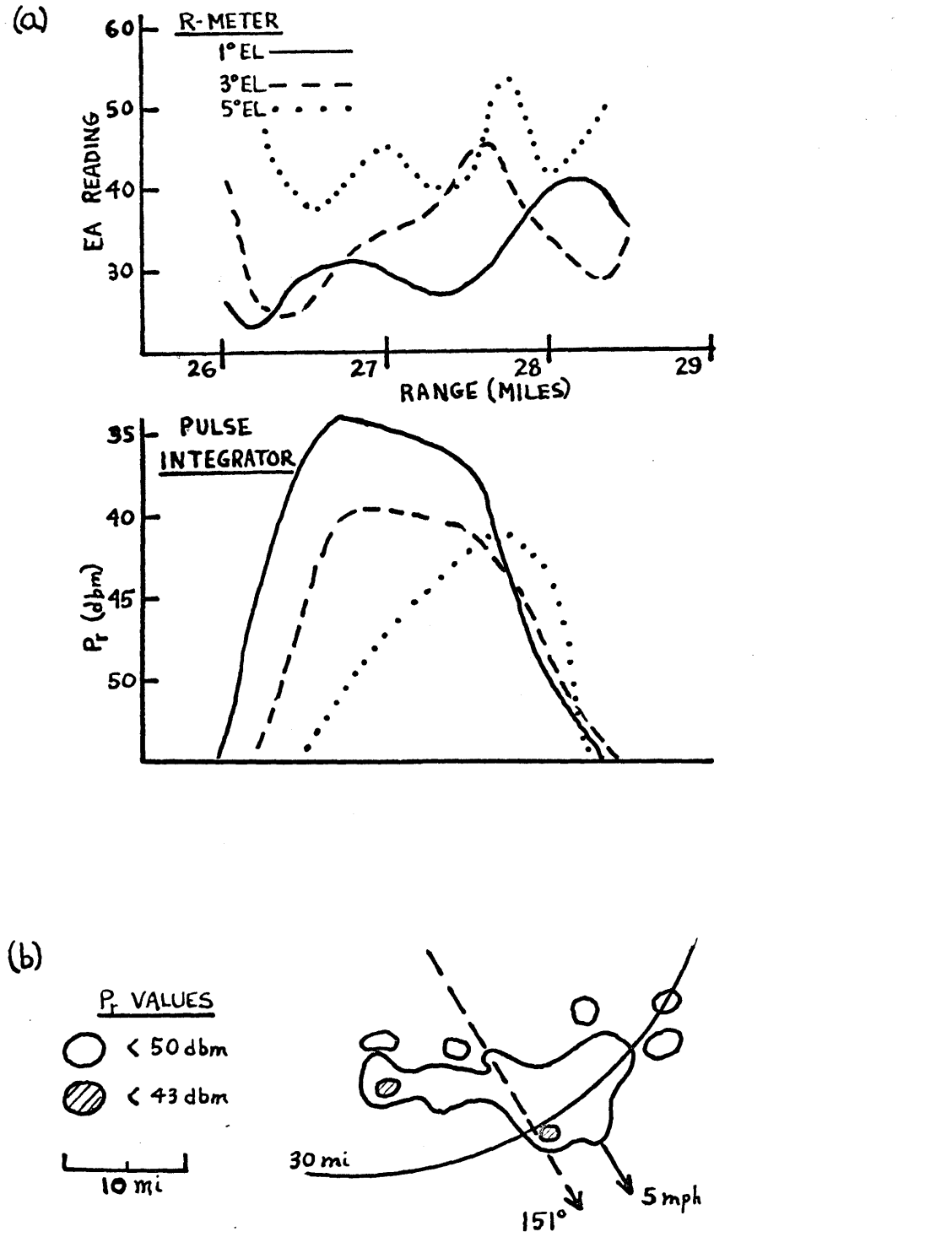

Figure 5. (a) Profiles for 23 July, 0928-0932 EST, 151° Azimuth. (b) PPI intensity contours at 0953 EST.

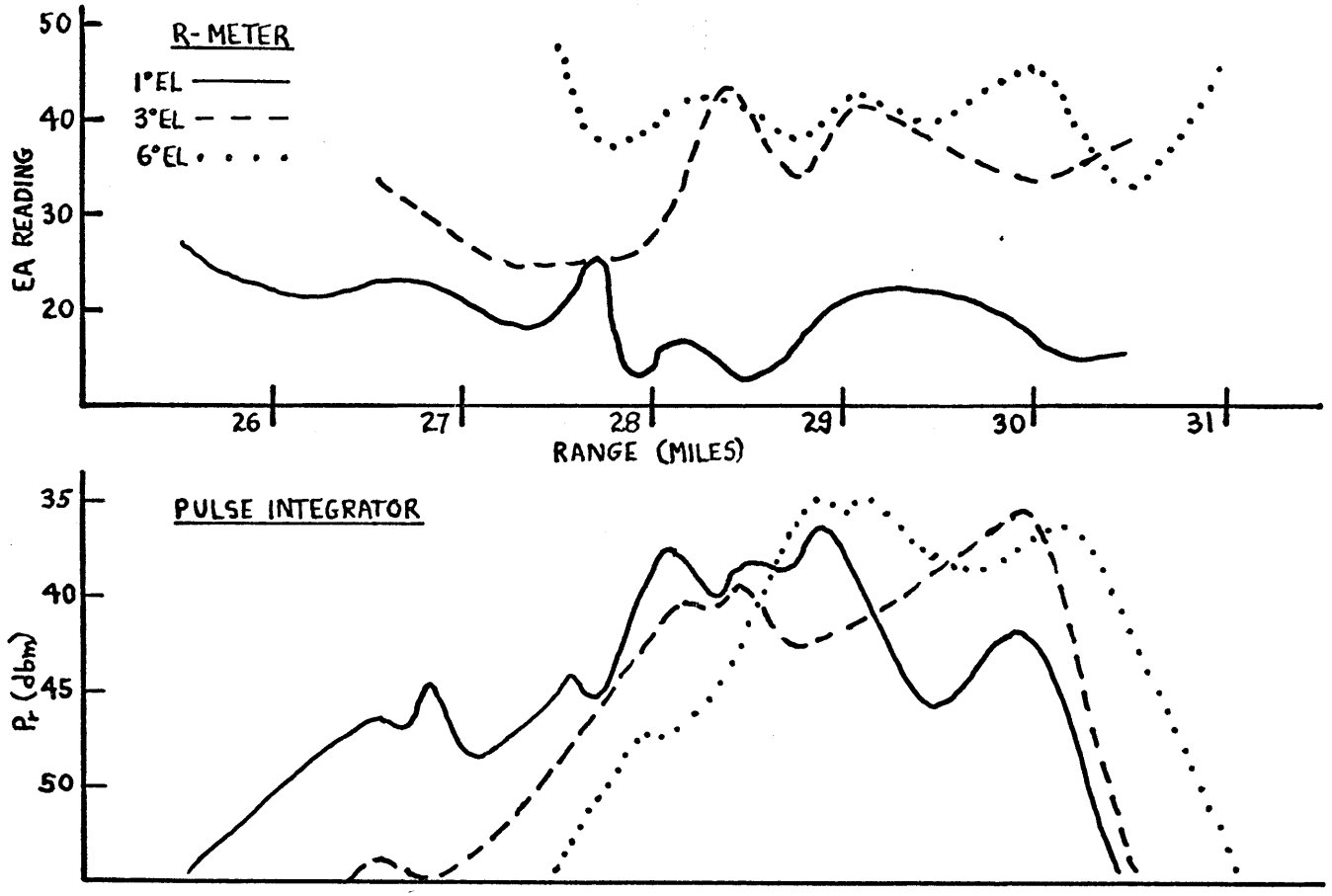

Figure 6a. Profiles for 23 July, 0940-0947 EST, 209° Azimuth. (See Figure 7a).

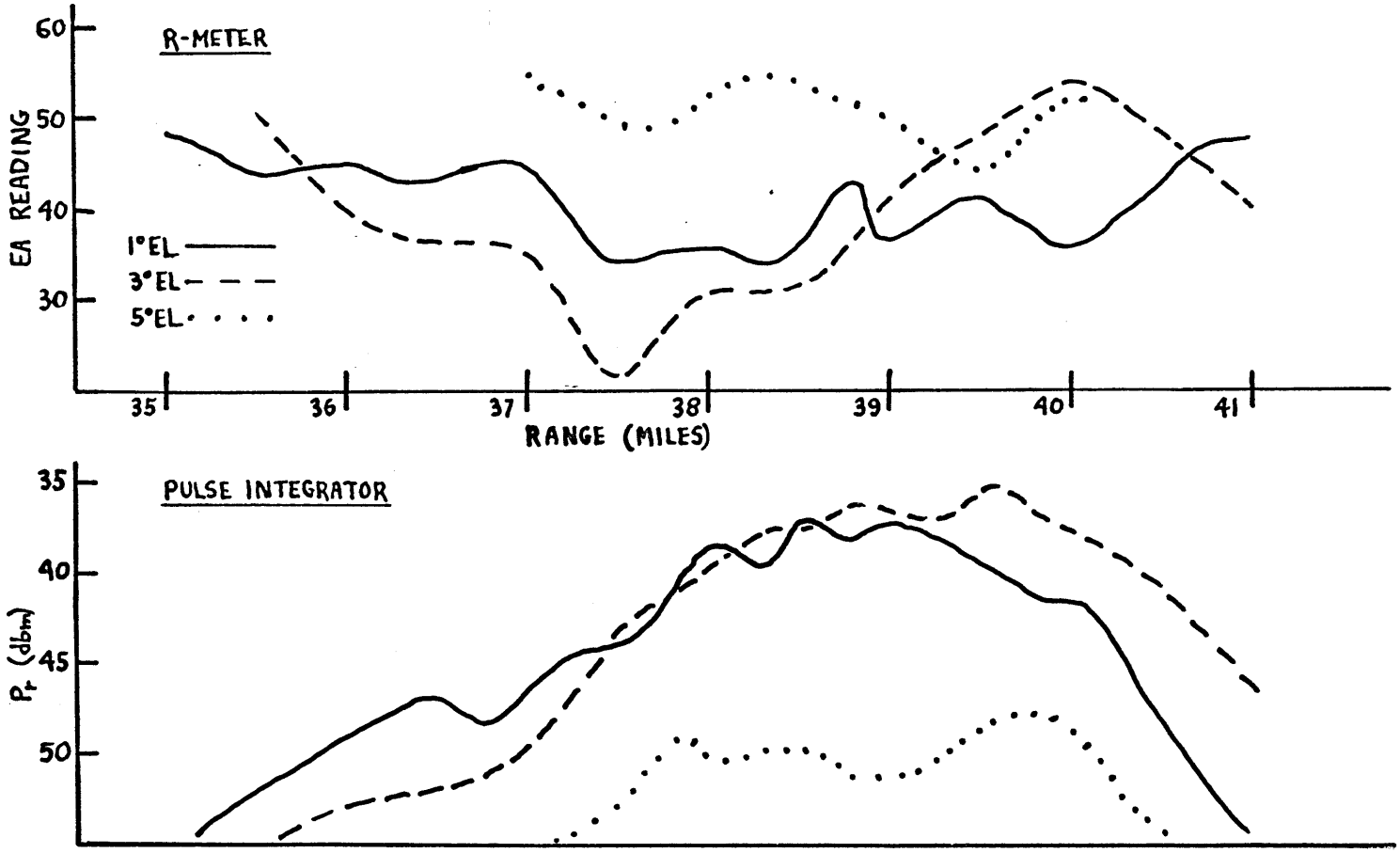

Figure 6b. Profiles for 23 July, 1141-1146 EST, 168° Azimuth. (See Figure 7b).

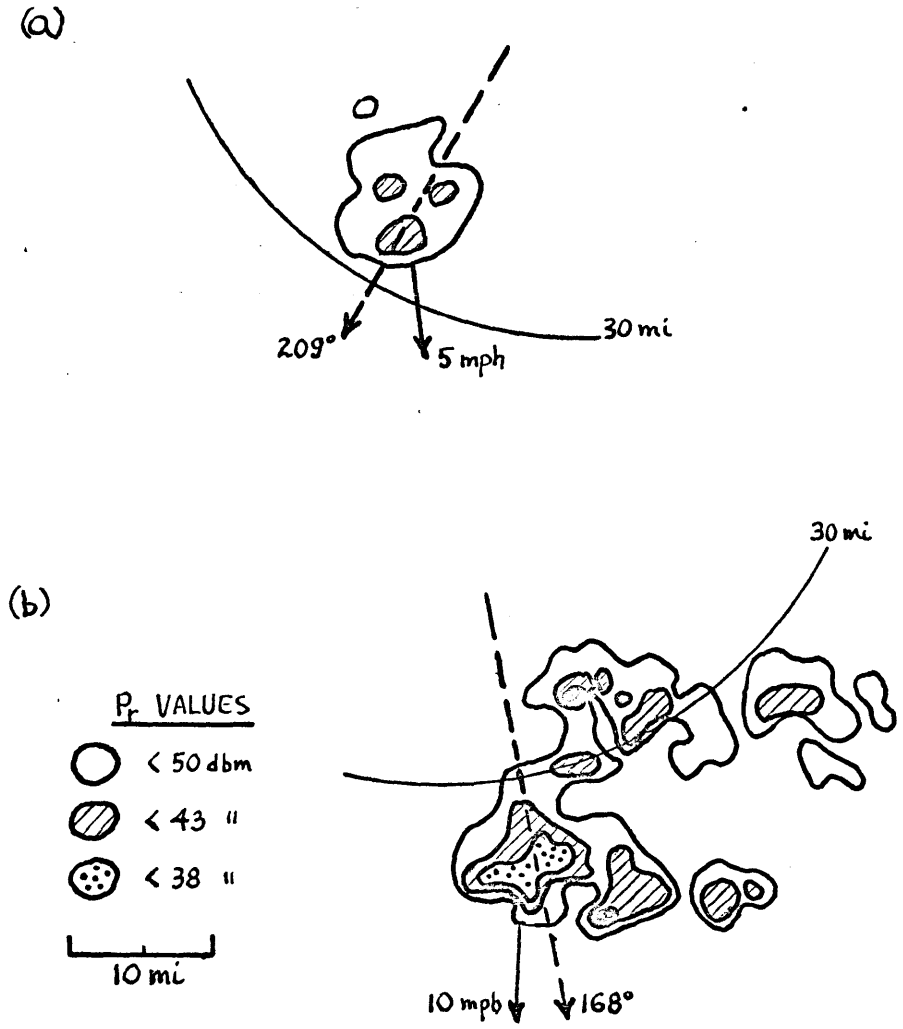

Figure 7. PPI Intensity Contours. (a) 23 July, 0953 EST. (b) 23 July, 1130 EST.

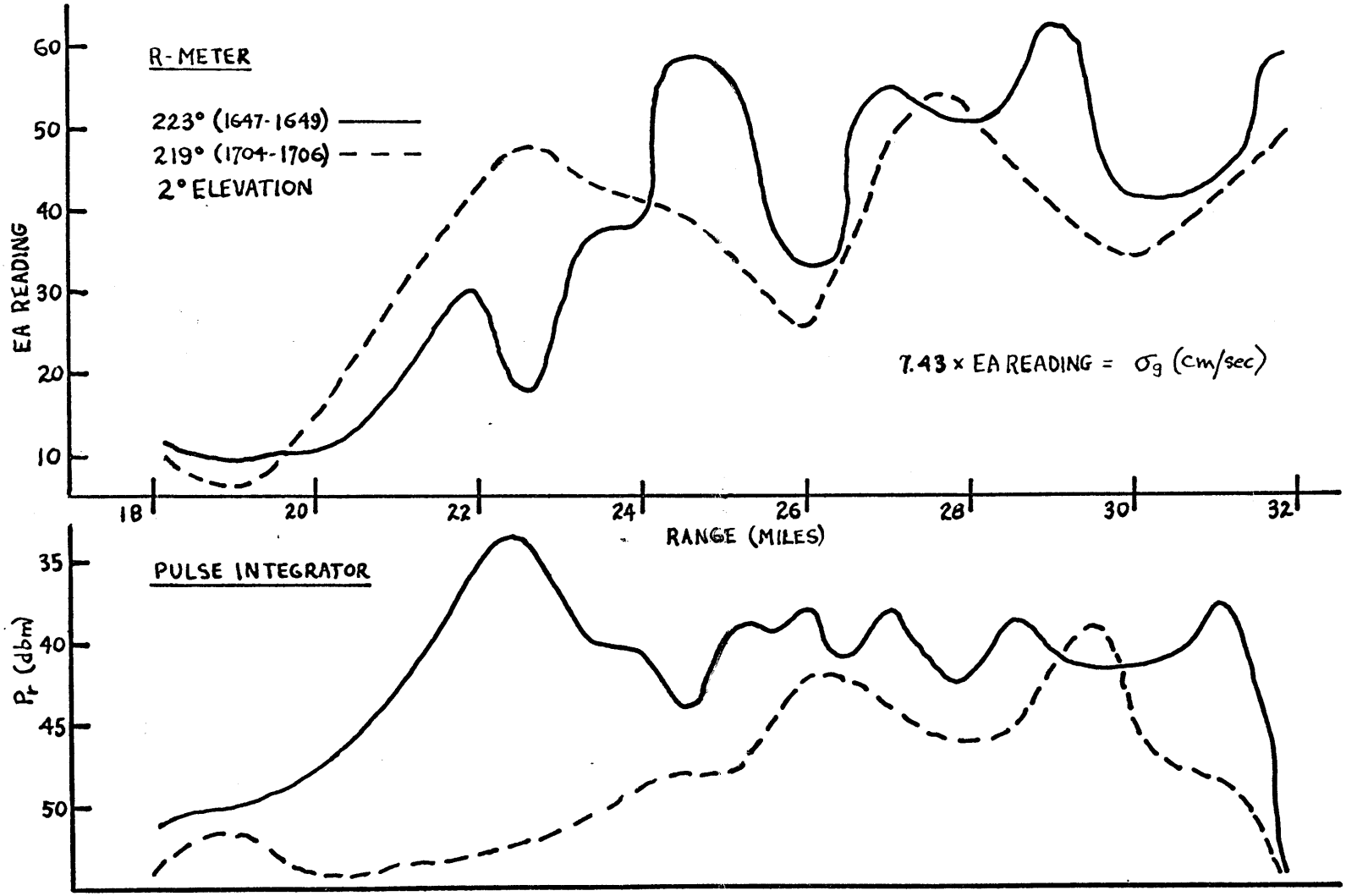

Figure 8a. Profiles for 8 August, 1647-1706 EST, 2° Elevation. Successive runs made through same line of echoes at same elevation. (See Figure 9a).

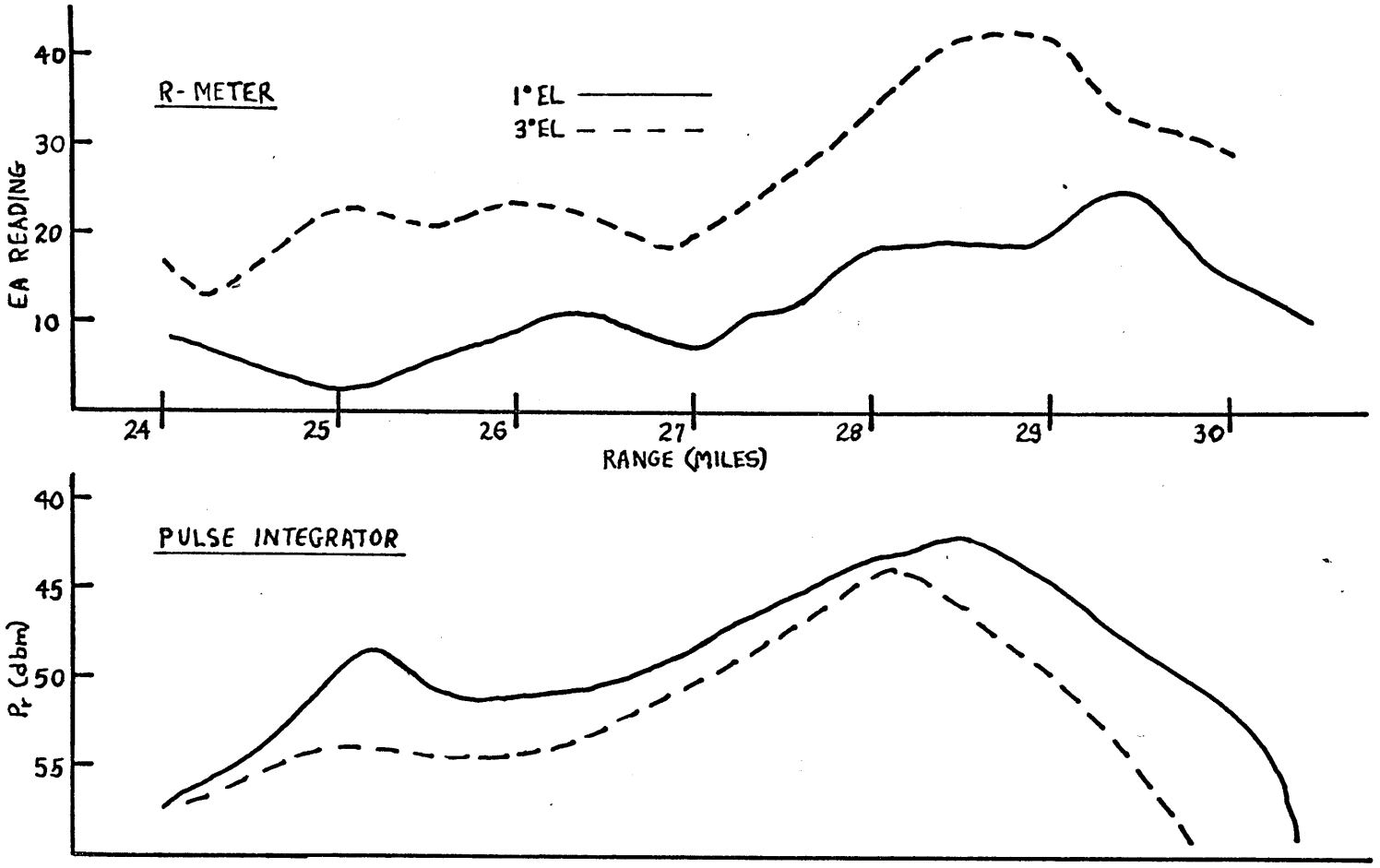

Figure 8b. Profiles for 18 August, 1520-1526 EST, 278° Azimuth. (See Figure 9b).

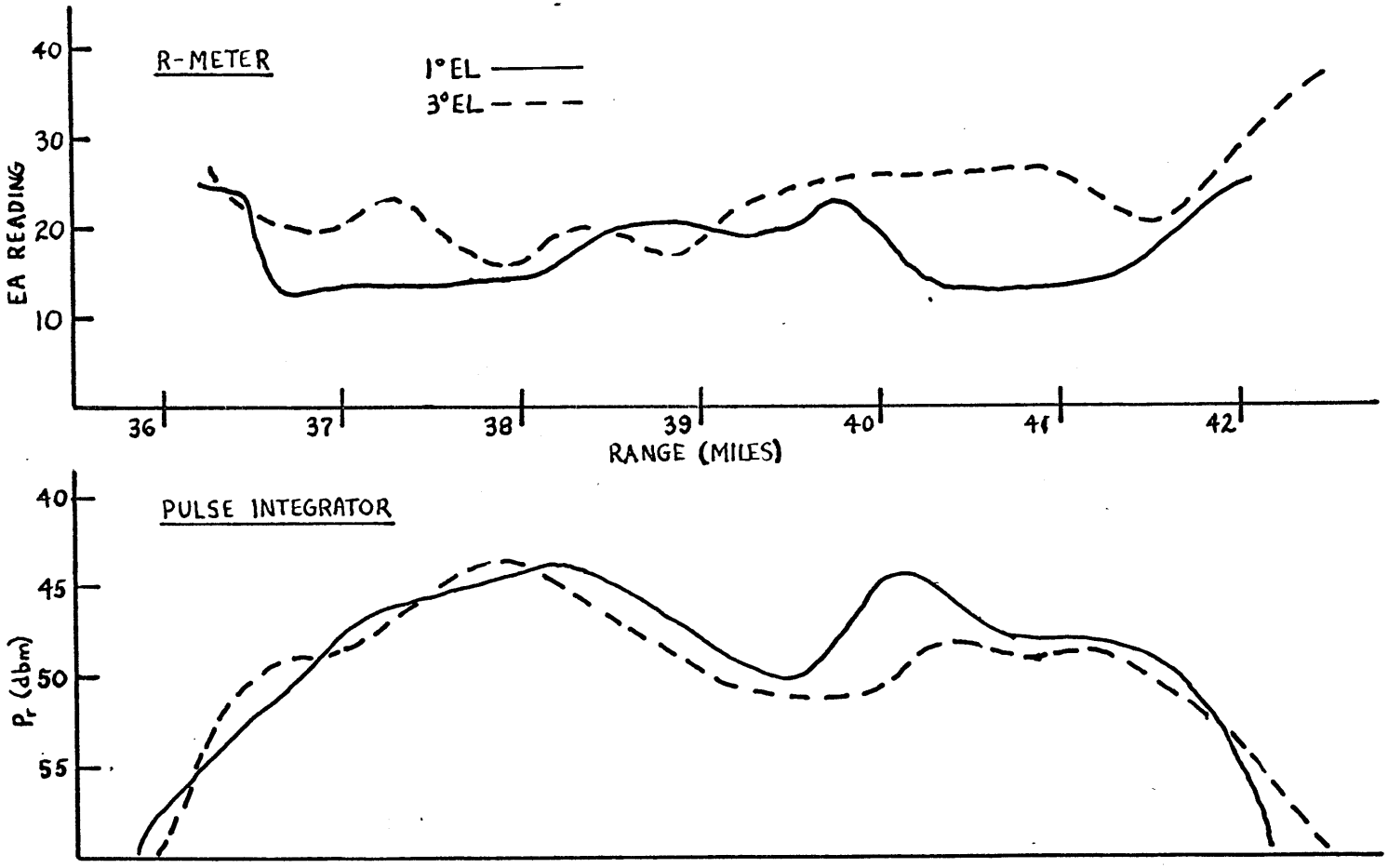

Figure 8c. Profiles for 12 August, 1342-1347 EST, 210° Azimuth. (See Figure 9c). Pr values may be converted to Ze values using 10 Log Ze = - Pr + 85. Equivalent rainfall rates, R, may be estimated by using $Ze \doteq 200R^{1.6}$ (R in mm/hr).

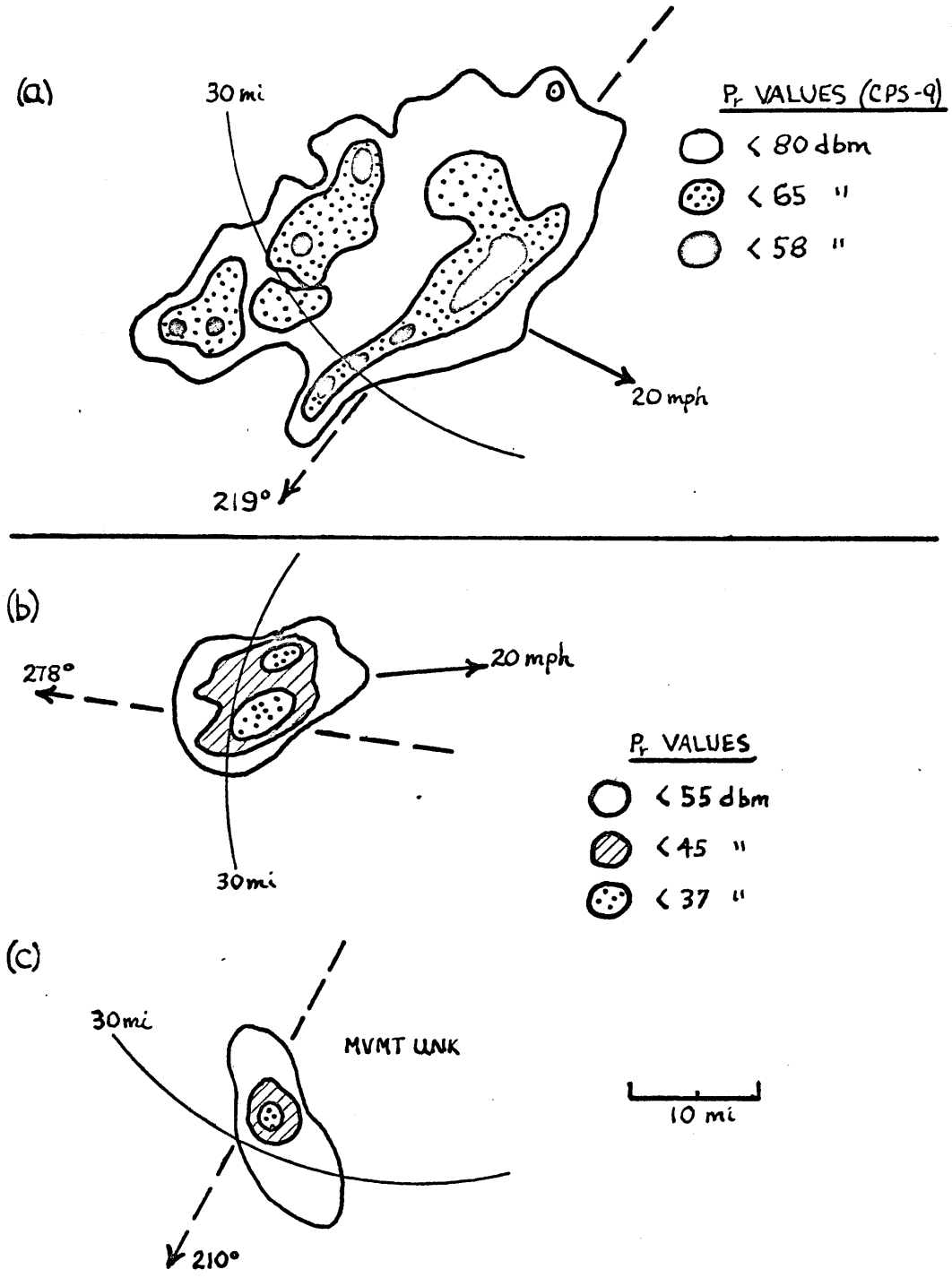

Figure 9. PPI intensity contours. (a) 8 August, 1705 EST. AN/CPS-9 short pulse was used in this one case. All other PPI contours were taken from SCR-615B data. Note the severe attenuation of the signal by comparing the simultaneous pulse integrator readings in Figure 8a. (b) 12 August, 1359 EST. (c) 18 August, 1516 EST.

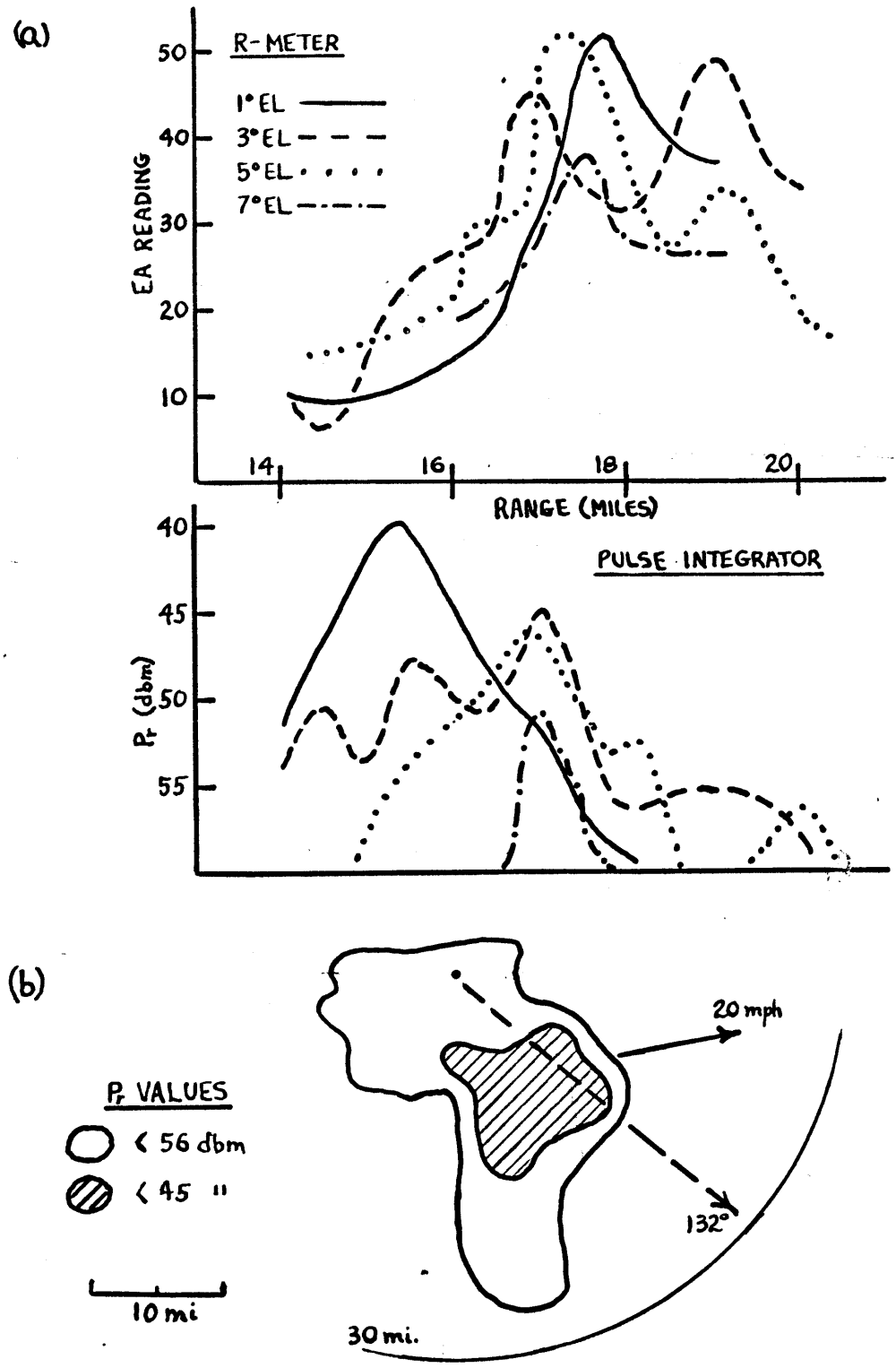

Figure 10. (a) Profiles for 18 August, 1700 EST, 132° Azimuth. (b) PPI intensity contours at 1700 EST.

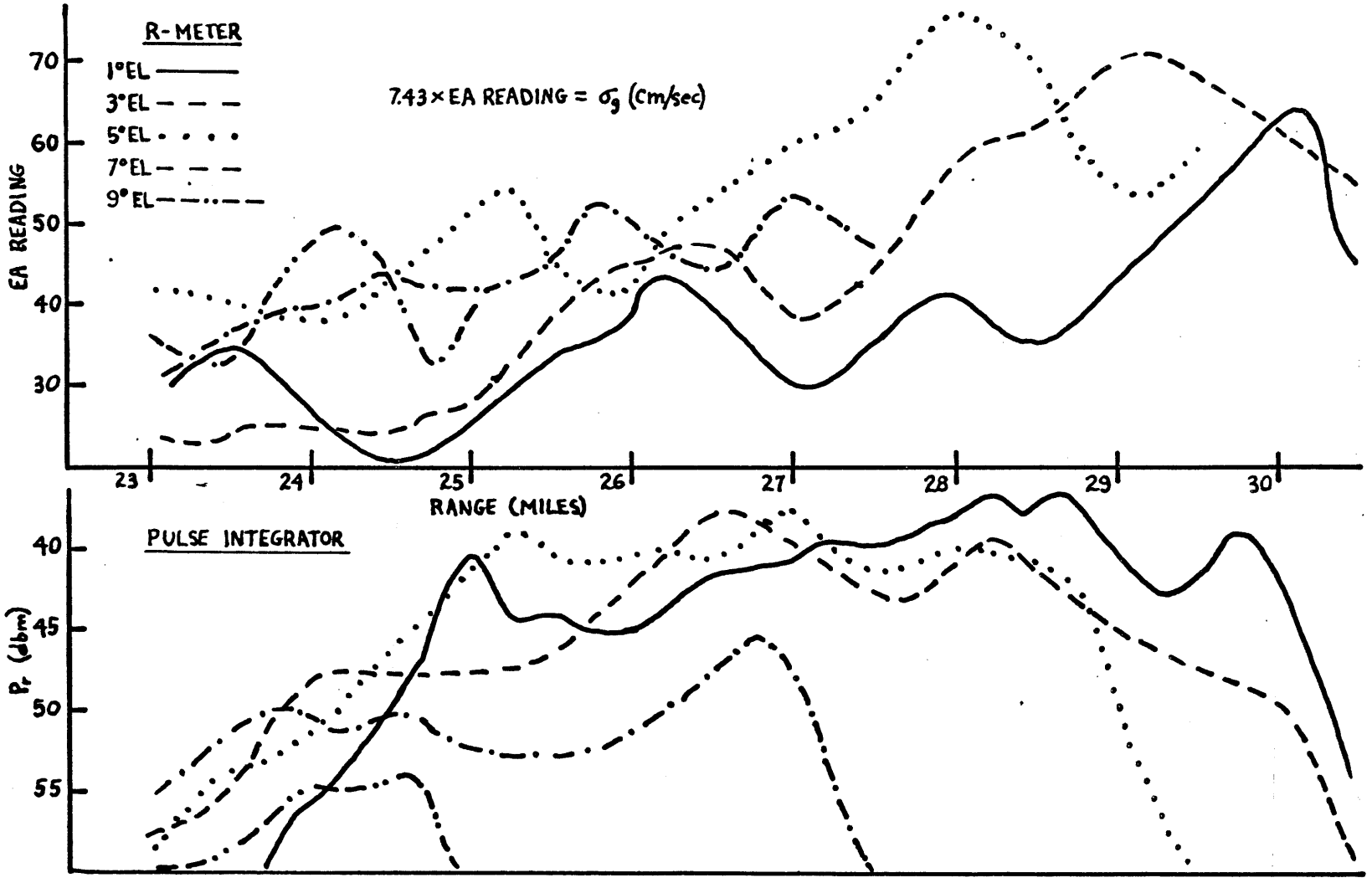

Figure 11a. Profiles for 26 August, 1150-1201 EST, 262° Azimuth. (See Figure 12a)

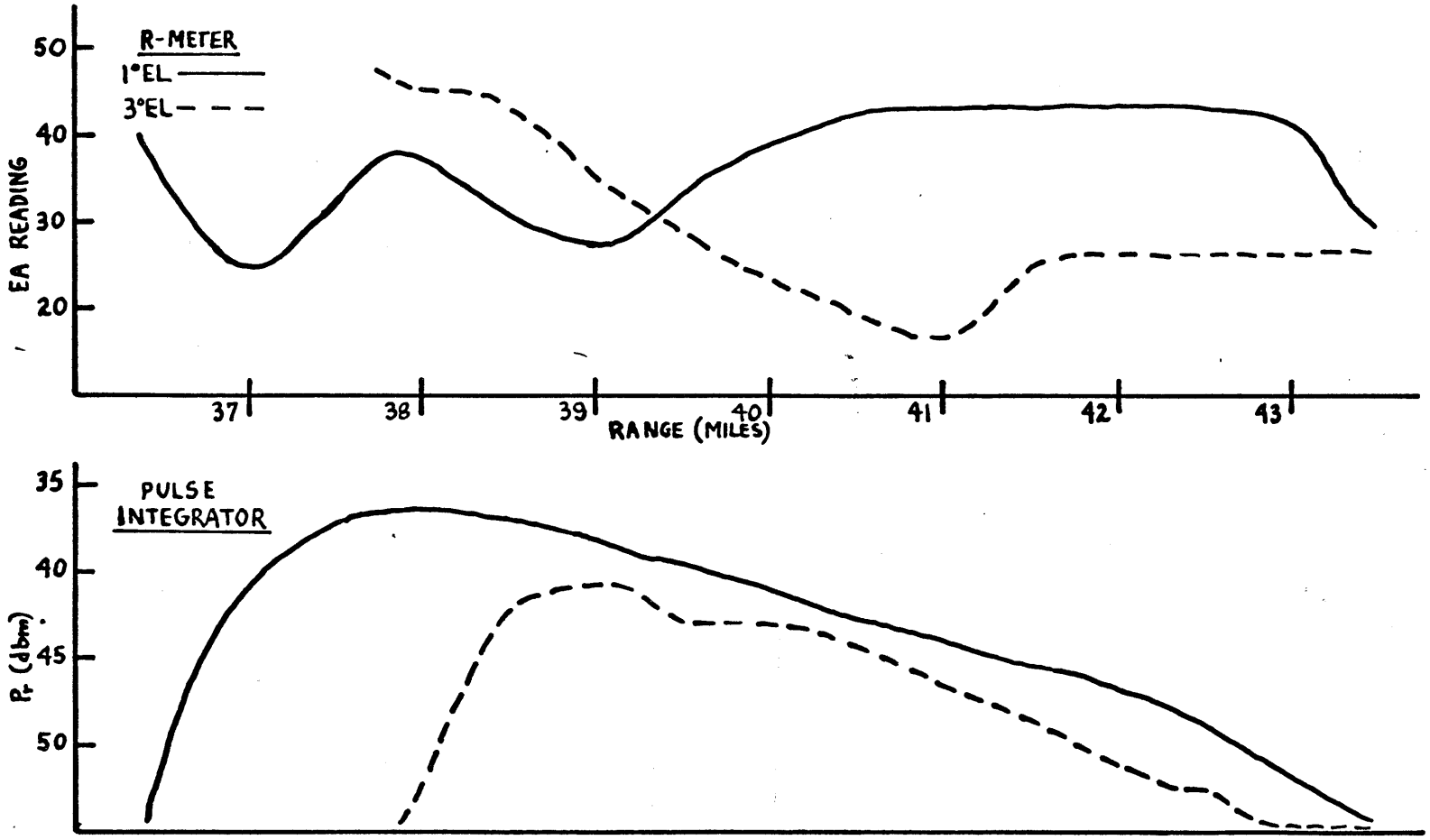

Figure 11b. Profiles for 26 August 1232-1239 EST, 029° Azimuth. (See Figure 12b)

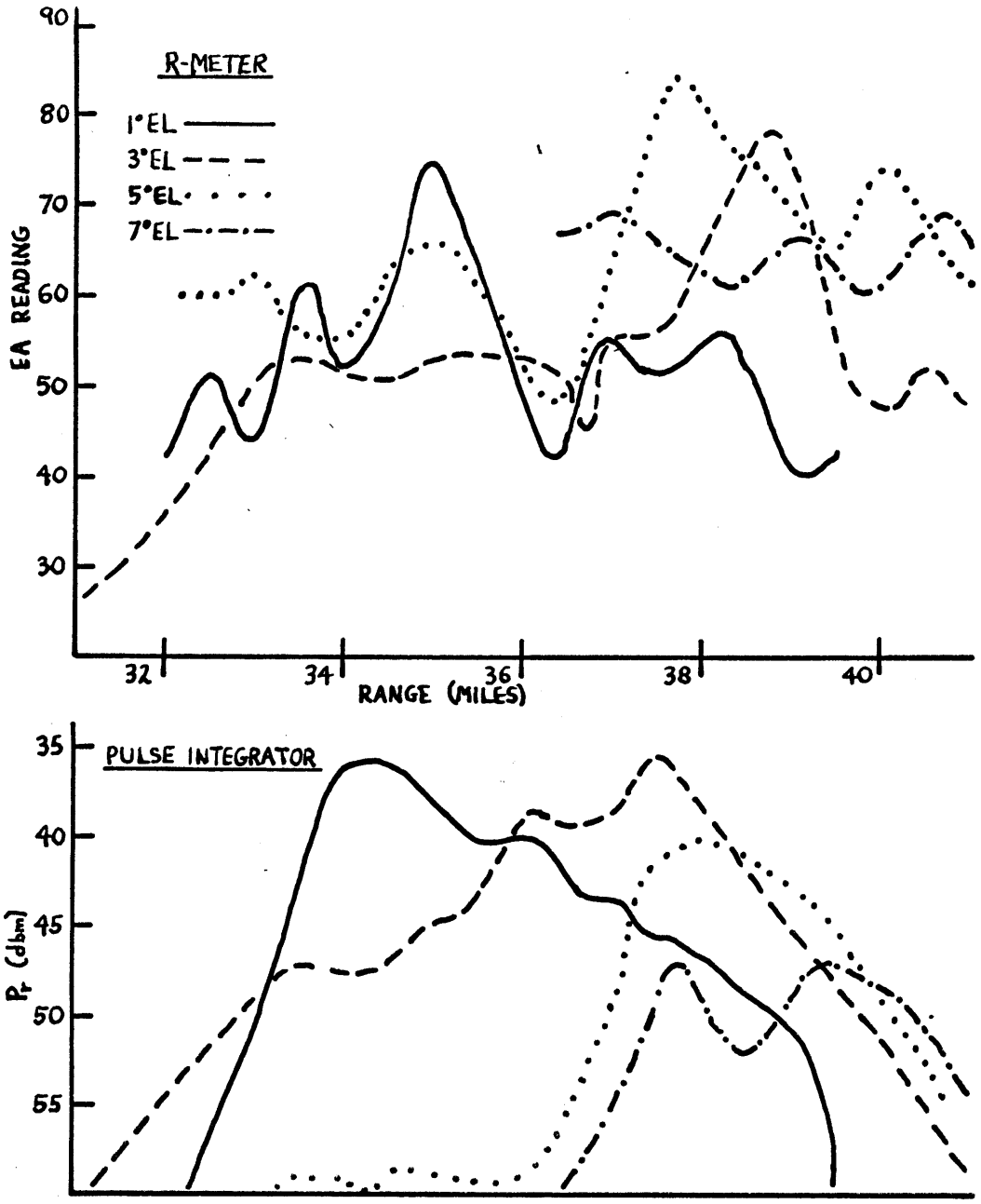

Figure 11c. Profiles for 26 August, 1350-1357 EST, 160° Azimuth. (See Figure 12c)

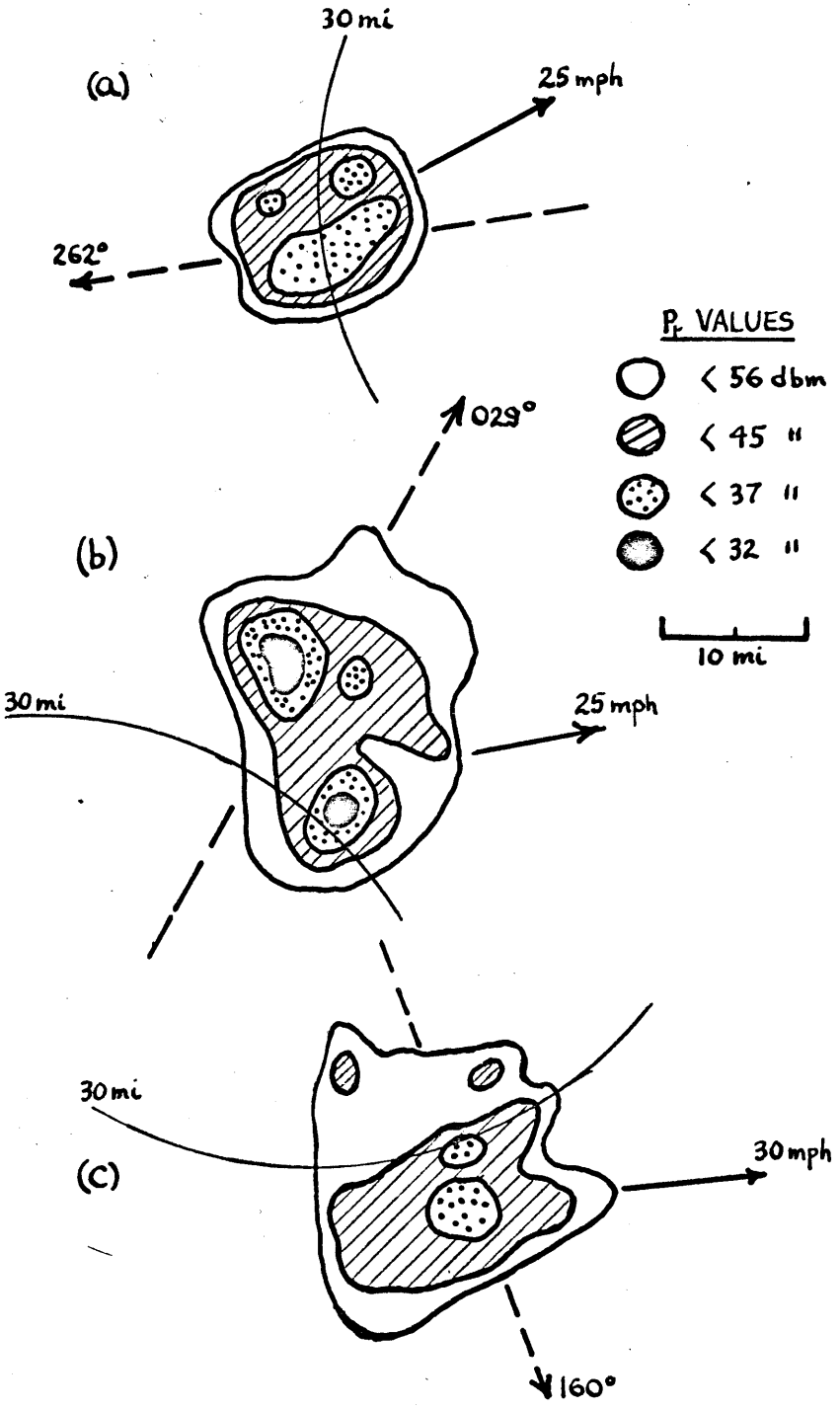

Figure 12. PPI intensity contours (a) 26 August, 1140 EST. (b) 26 August, 1230 EST. (c) 26 August, 1345 EST.

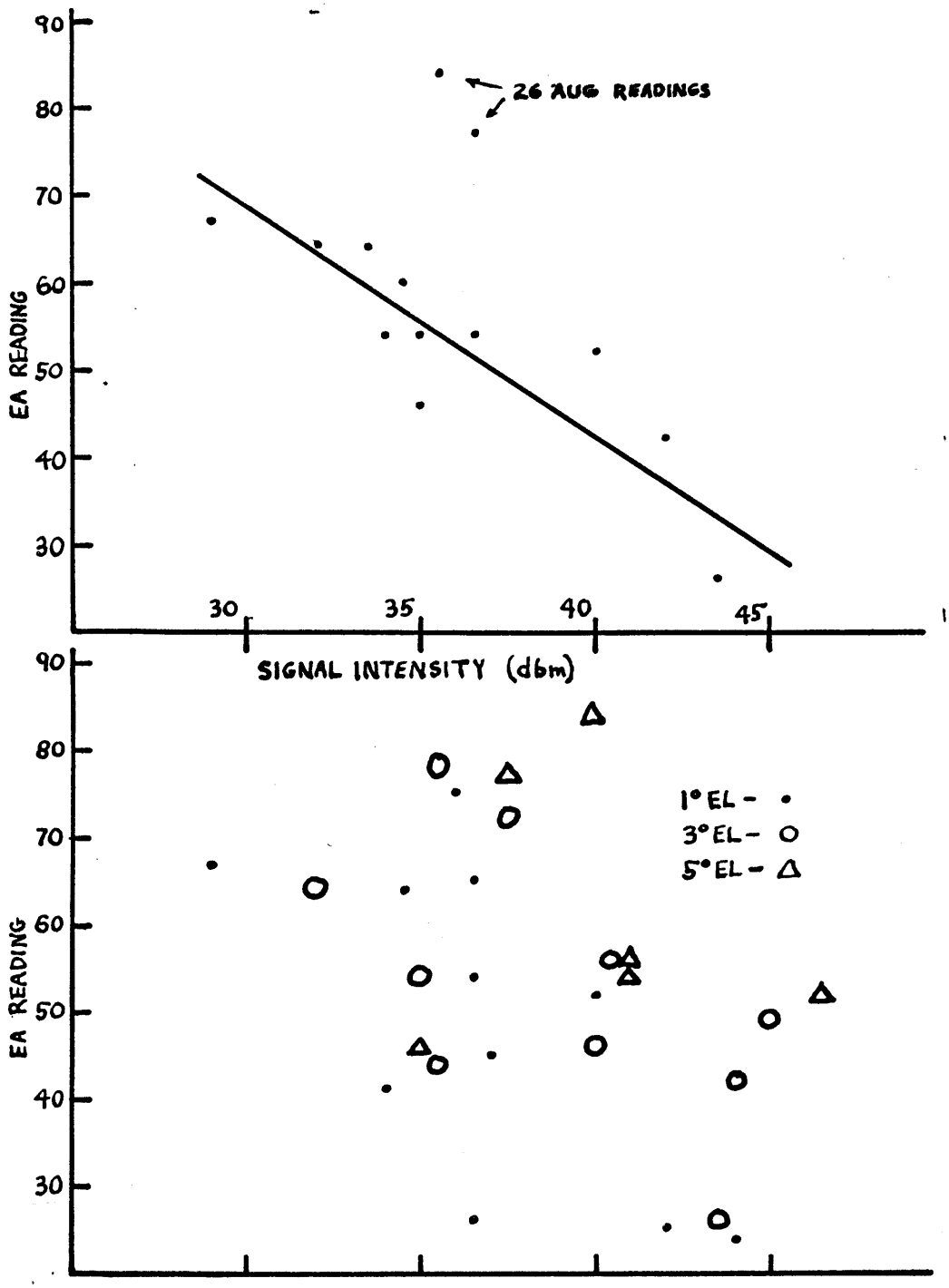

Figure 13. (a) Maximum R-meter readings at any level versus maximum signal intensities at any level through the same storms. (b) Maximum R-meter readings versus maximum signal intensities at individual levels.

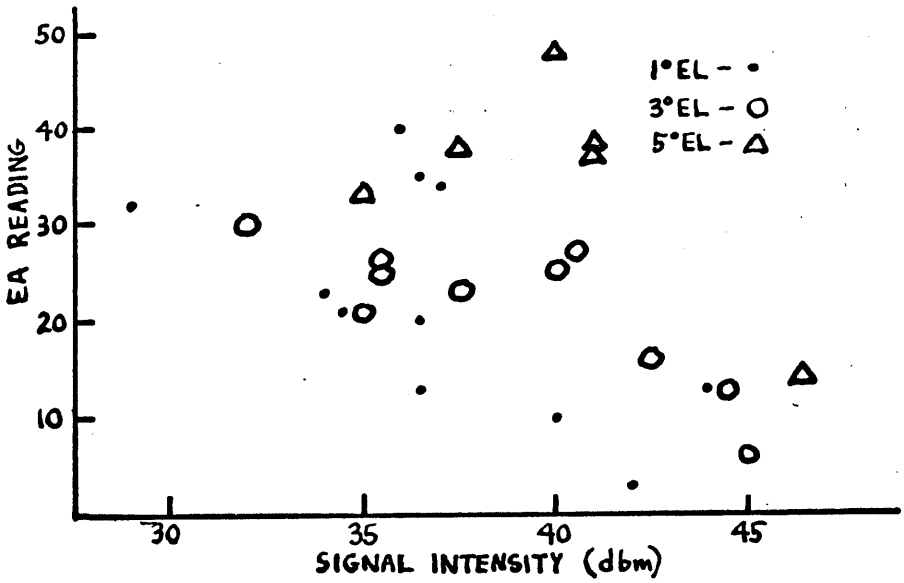

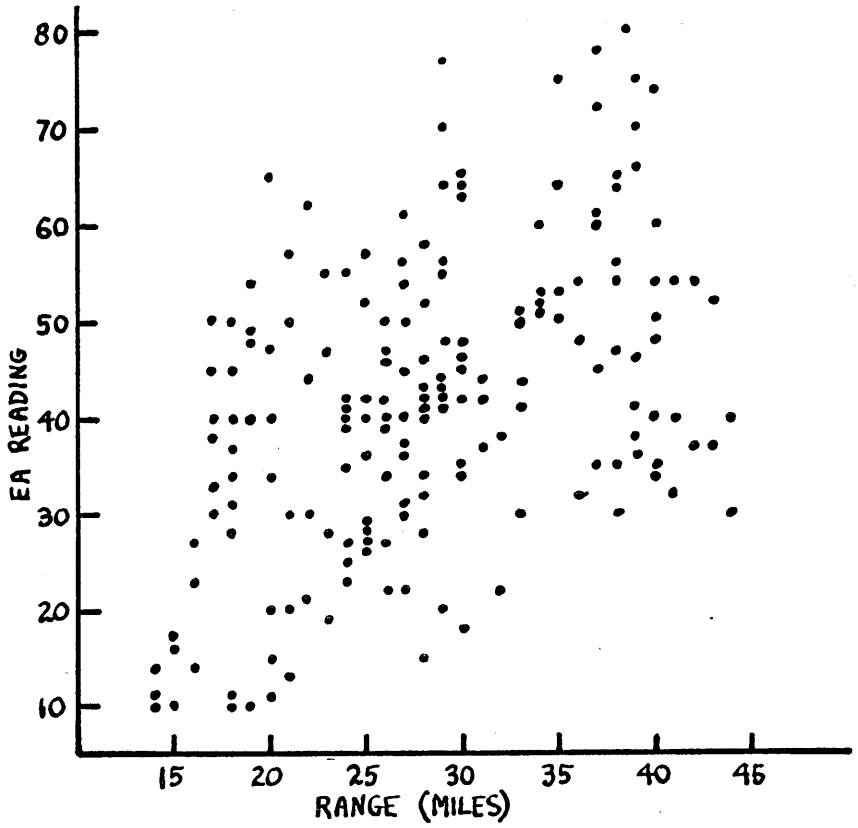

Figure 14. (a) Minimum R-meter readings versus maximum signal intensities at individual levels. (b) R-meter readings versus range at one mile increments for all readings above receiver noise level.

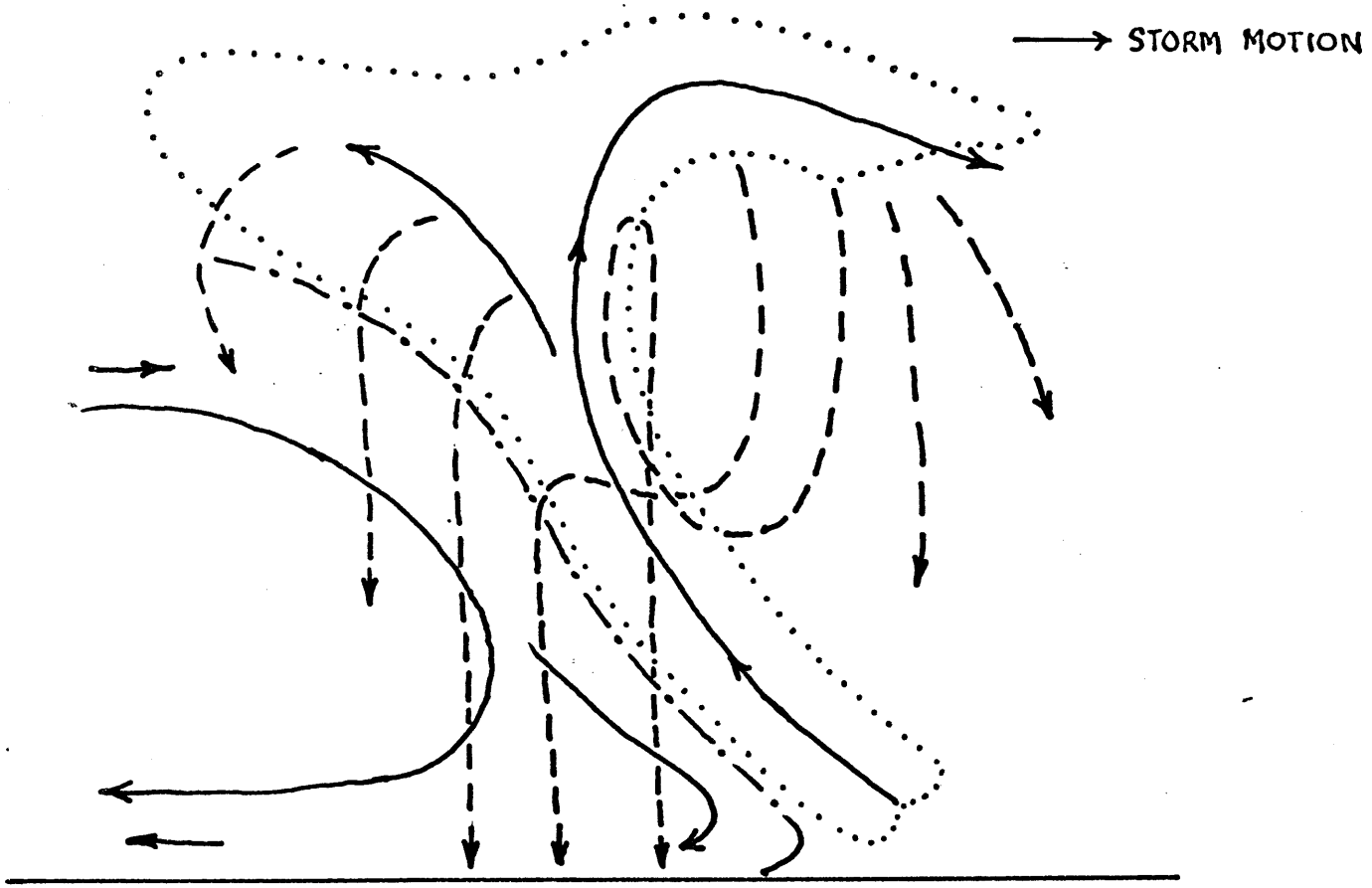

Figure 15. Model of middle latitude cumulonimbus; condensation occurring within dotted area, some paths of precipitation particles indicated by dashed lines. (From Ludlam, 1963)

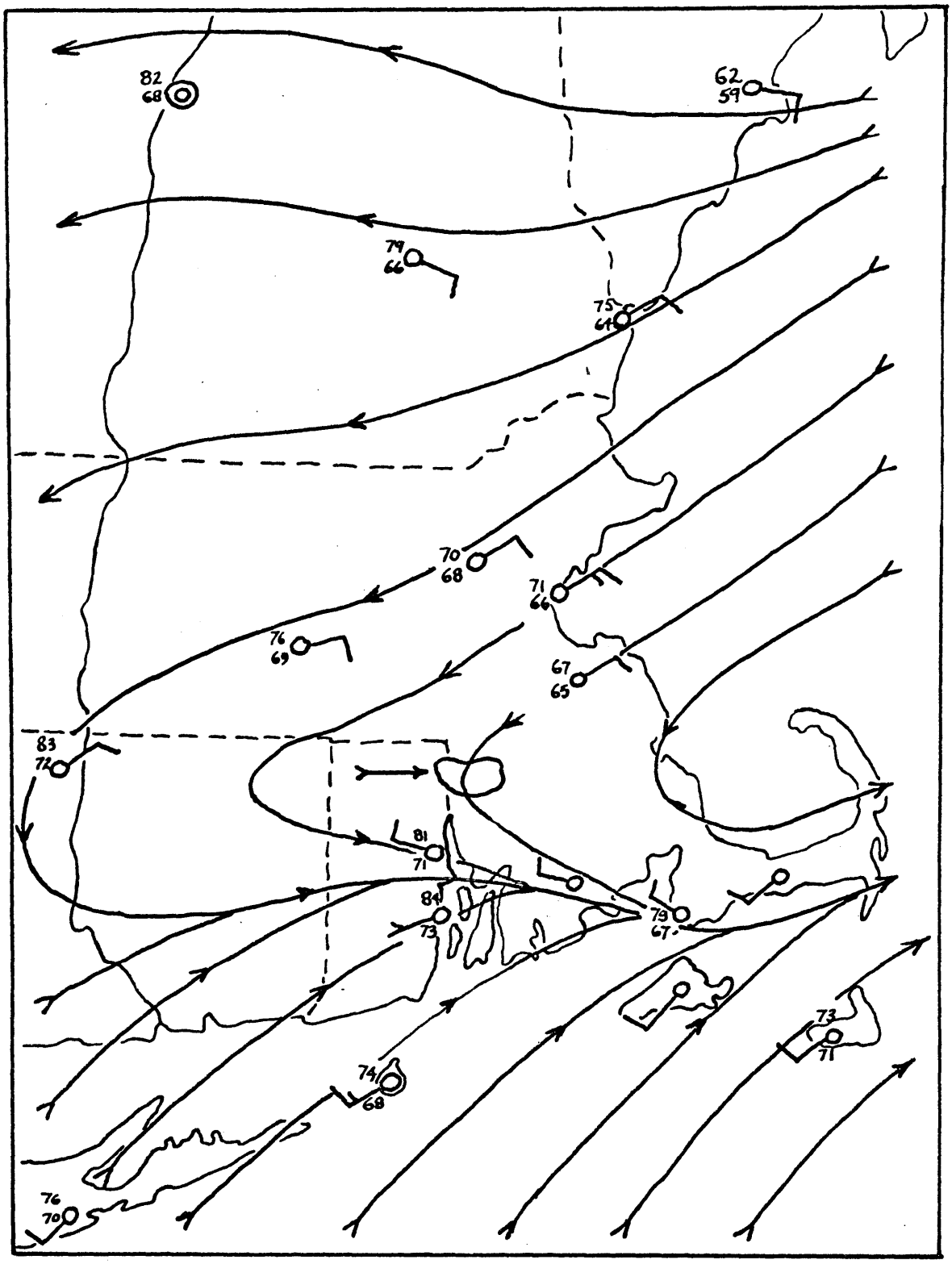

Figure 16. Surface Streamlines for 23 July, 1100 EST with position of radar echo for case study indicated by arrow.

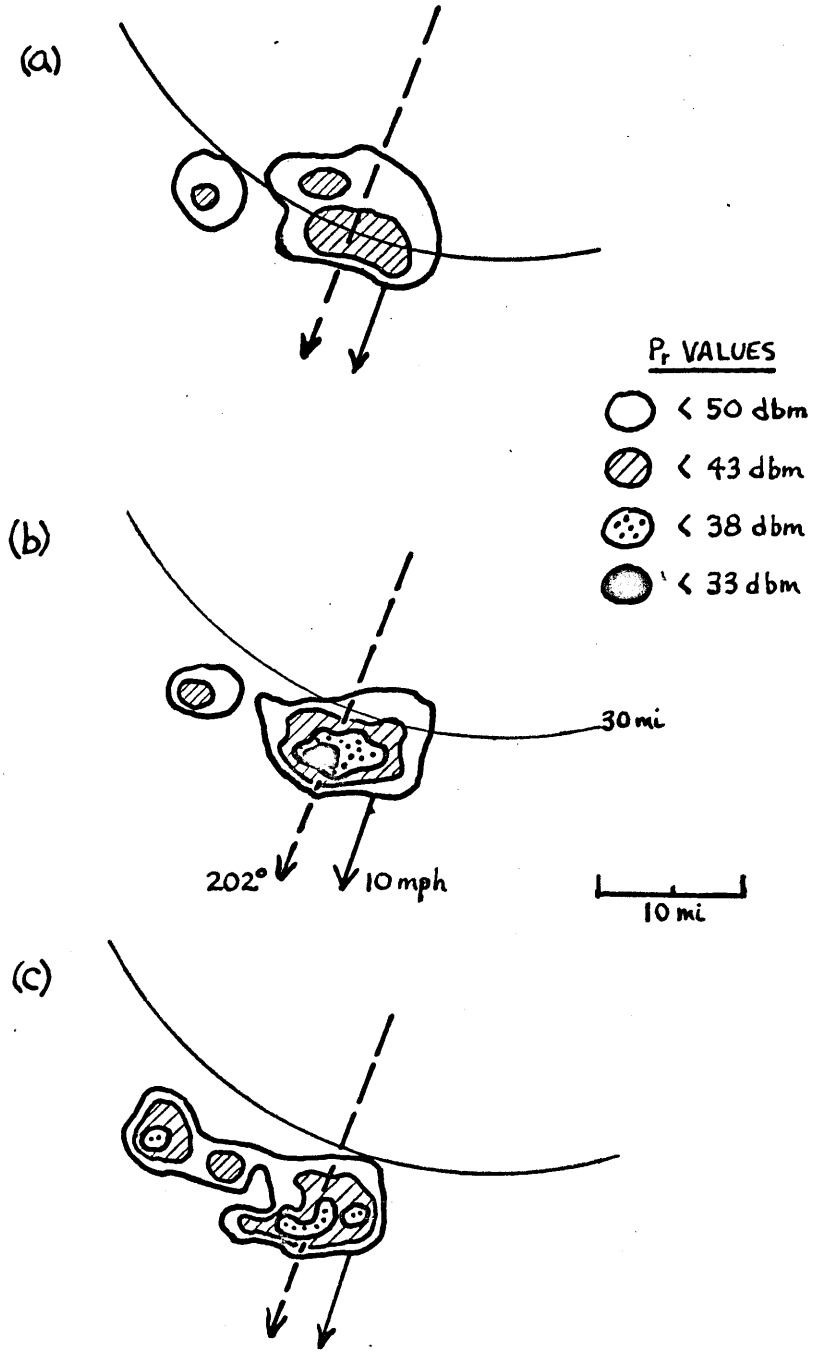

Figure 17. PPI intensity contour. (a) 23 July, 1040 EST. (b) 23 July, 1045 EST. (c) 23 July, 1102 EST.

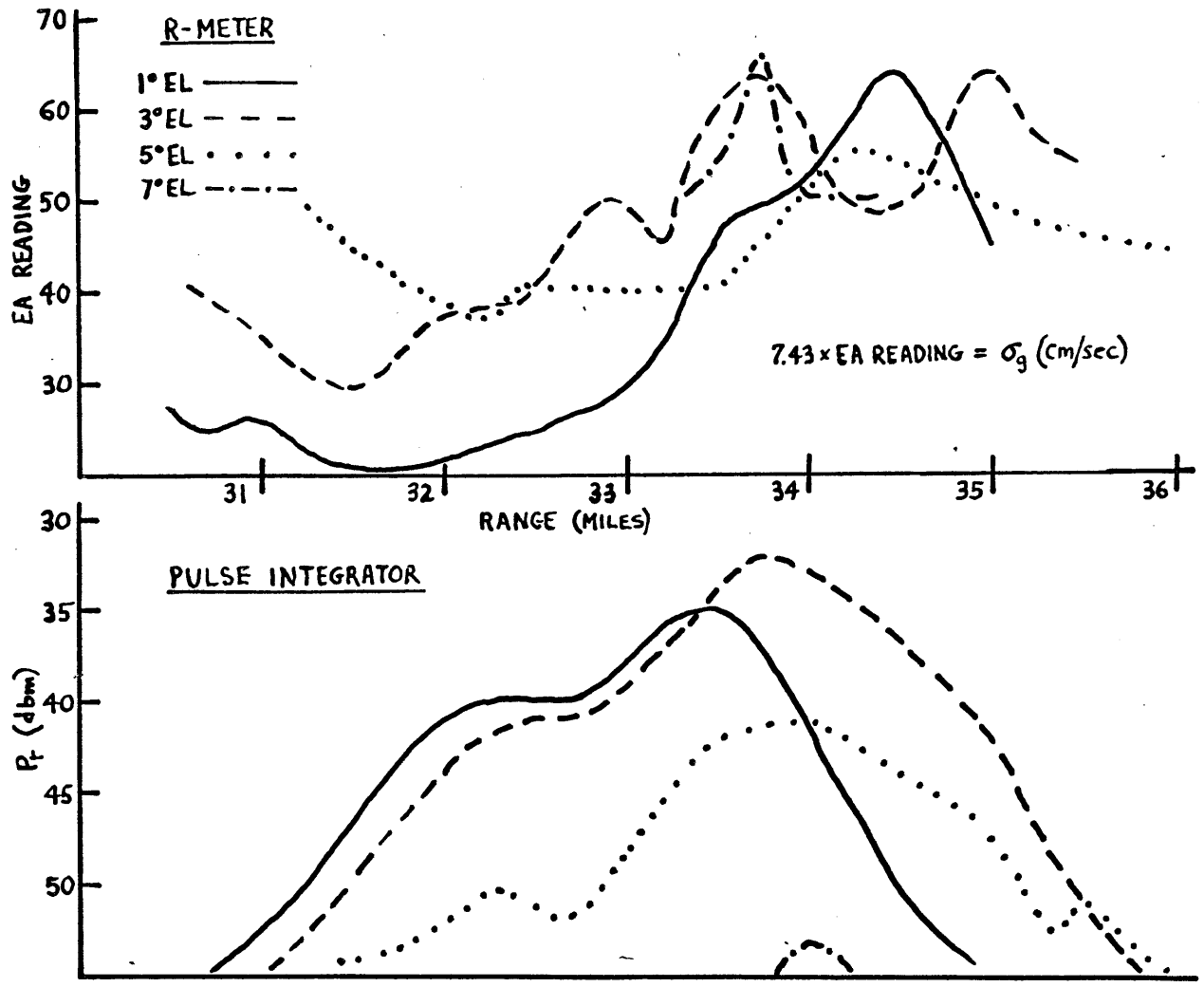

Figure 18. Profiles for 23 July, 1050–1058 EST, 202° Azimuth. (See Figure 17), Pr may be converted to Ze using 10 log Ze = – Pr + 85. Equivalent rainfall rates, R, may be estimated from, $Ze = 200R^{1.6}$.

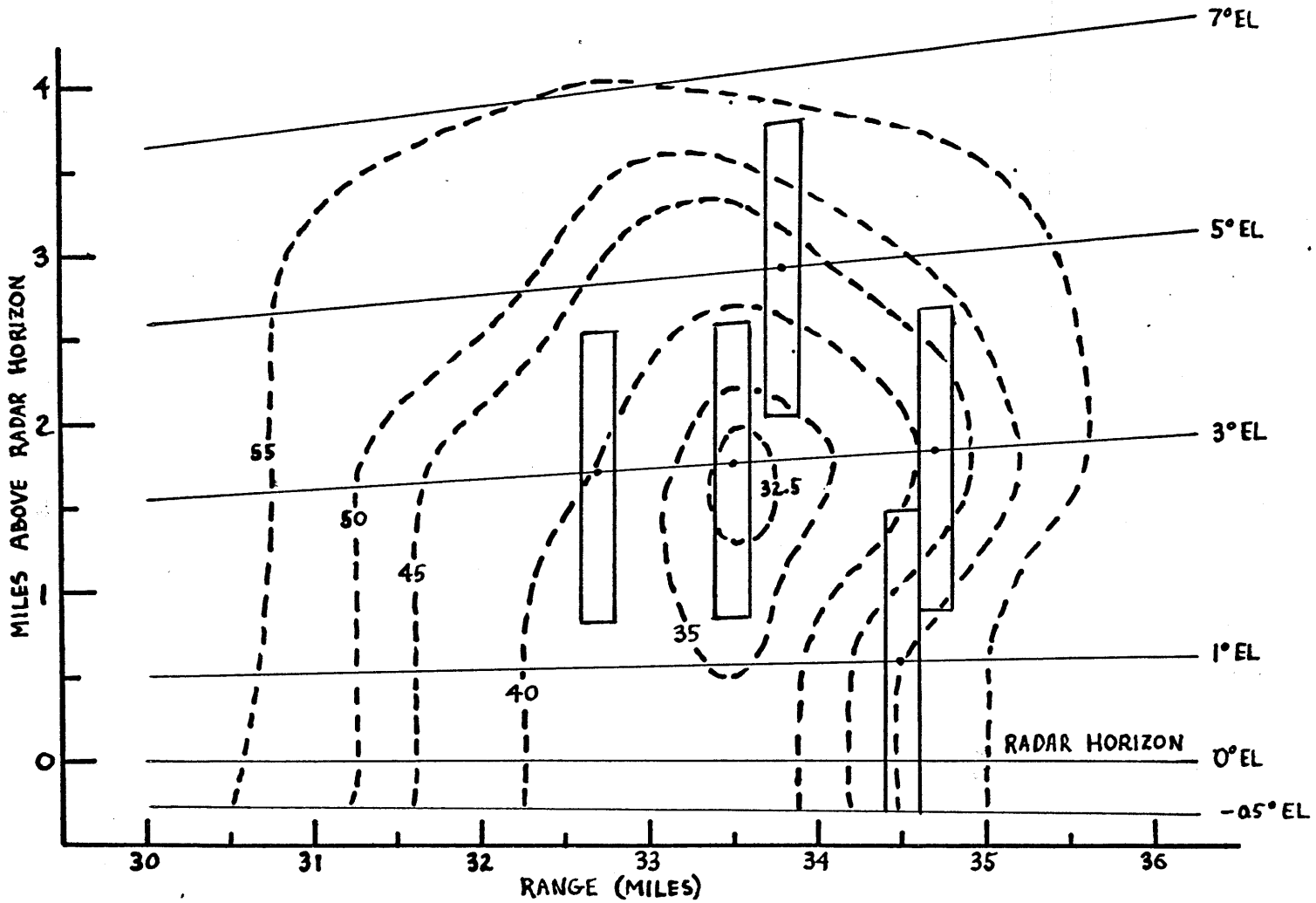

Figure 19a. Cell Structure of 23 July storm (1050 EST) built by joining points of equal signal intensity (dbm) at each elevation angel in 5 db intervals. Upright rectangles are side views of sampling volumes at the points where peaks in the R-meter traces occurred.

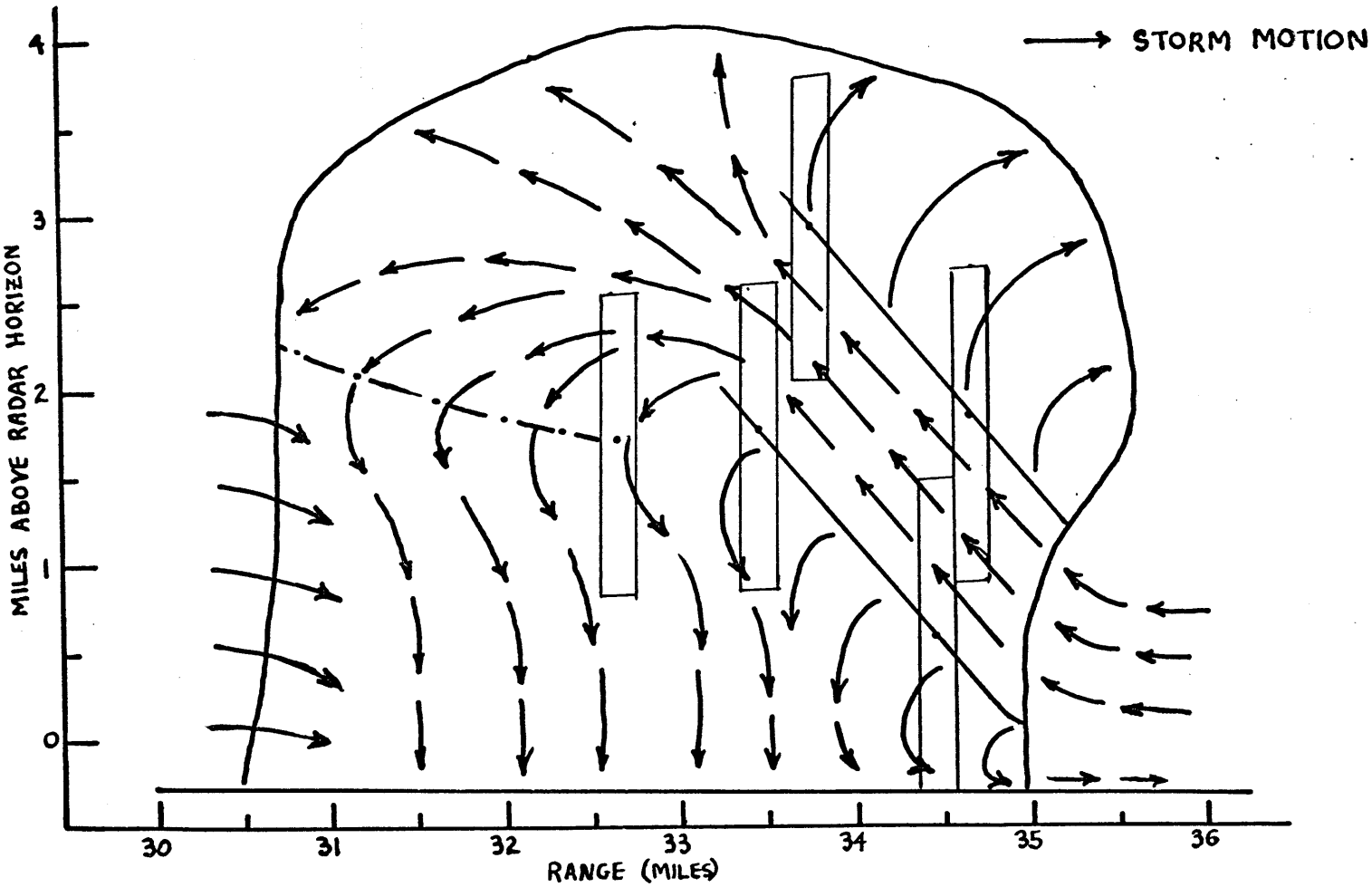

Figure 19b. Cell circulation of 23 July storm (1050 EST) deduced from positions of R-meter peaks (upright rectangles) See Discussion of the Data, Part B. for complete explanation of model.